

---

# Uncertainty Quantification for Large Language Diffusion Models

---

Artem Vazhentsev<sup>1</sup> Vladislav Smirnov<sup>1</sup> David Li<sup>1</sup>  
Maxim Panov<sup>1</sup> Timothy Baldwin<sup>1,2</sup> Artem Shelmanov<sup>1</sup>

<sup>1</sup>MBZUAI <sup>2</sup>The University of Melbourne

artem.vazhentsev@mbzuai.ac.ae artem.shelmanov@mbzuai.ac.ae

## Abstract

Large Language Diffusion Models (LLDMs) are emerging as an alternative to autoregressive models, offering faster inference through higher parallelism. Similar to autoregressive LLMs, they remain prone to hallucinations, making reliable uncertainty quantification (UQ) crucial for safe deployment. However, existing UQ methods are fundamentally misaligned with this new paradigm: they assume autoregressive factorization or use expensive repeated sampling, negating the efficiency of LLDMs. In this work, we present the first systematic study of UQ for LLDMs and propose lightweight, zero-shot uncertainty signals derived from the iterative denoising process, leveraging intermediate generations, token remasking dynamics, and denoising complexity. We further adapt a state-of-the-art UQ method to LLDMs by combining masked diffusion likelihoods with trajectory-based semantic dissimilarity. We prove that expected trajectory dissimilarity lower bounds the masked diffusion training objective, which motivates its usage as an uncertainty score. Comprehensive experiments across three tasks, eight datasets, and two models show that our method achieves a great cost-performance trade-off: it approaches the strongest sampling-based baselines while incurring up to 100x lower computational overhead. Our work demonstrates that LLDMs can deliver both fast inference and reliable hallucination detection simultaneously.

## 1 Introduction

Large language models (LLMs) are known to hallucinate (Huang et al., 2025), producing fluent but factually incorrect outputs, making reliable uncertainty quantification (UQ) a critical problem (Kuhn et al., 2023). While most prior work on UQ has focused on autoregressive models, Large Language Diffusion Models (LLDMs) have recently emerged as a competitive alternative (Ye et al., 2025; Nie et al., 2025; Bie et al., 2025), offering faster generation through semi-autoregressive decoding, where multiple tokens within a block are generated in parallel and iteratively refined (Wu et al., 2026).

However, existing UQ methods are misaligned with this diffusion-based paradigm. Standard approaches are either tailored to token-by-token autoregressive generation (Malinin and Gales, 2021) or computationally expensive due to repeated sampling (Duan et al., 2024; Vashurin et al., 2025b), making them poorly suited for LLDMs, where efficiency is the main objective (Sahoo et al., 2026a).

In this work, we investigate diffusion-specific signals for UQ and introduce uncertainty measures that exploit diffusion trajectories, masking dynamics, and generation complexity, as illustrated in Figure 1. These signals enable principled UQ that is both effective and efficient. Our results show that LLDMs offer a dual advantage: fast inference and reliable UQ, without relying on the costly sampling procedures typically required by autoregressive UQ methods (Vashurin et al., 2025a).

We summarize our main **contributions** as follows:

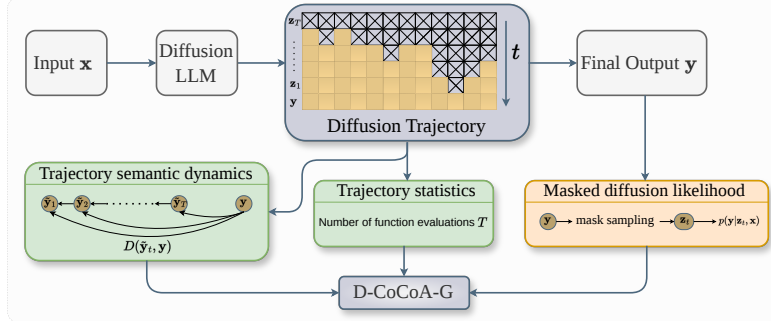


Figure 1: An illustration of the proposed D-CoCoA-G method. Given a prompt  $\mathbf{x}$ , the LLM generates an output  $\mathbf{y}$  via iterative denoising states  $\mathbf{z}_T, \dots, \mathbf{z}_1$ . D-CoCoA-G scores combines three diffusion-specific signals: (1) trajectory semantic instability, measuring semantic dissimilarity  $D(\tilde{\mathbf{y}}_t, \mathbf{y})$  between  $\arg \max$ -decoded intermediate states and the final output; (2) trajectory statistics, capturing generation complexity through the number of function evaluations; and (3) masked diffusion likelihood, approximating the conditional log-likelihood.

1. **Diffusion-specific uncertainty signals.** We introduce a set of novel uncertainty signals tailored to LLMs, including trajectory semantics instability, trajectory statistics, and re-masking behavior.
2. **Theoretical grounding.** We formally show that expected trajectory dissimilarity, one of the strongest UQ signals introduced in this work, is a principled surrogate for the discrete masked diffusion training objective, which motivates its usage as an uncertainty score.
3. **D-CoCoA: an effective and efficient UQ method for LLMs.** We adapt CoCoA, a state-of-the-art UQ method, to LLMs by replacing its log-likelihood component with a diffusion-aware surrogate and its sampling-based component with intermediate states generated along the denoising trajectory, yielding a method that is both effective and efficient.
4. **First large-scale systematic empirical study of UQ for LLMs.** We conduct experiments across diverse tasks and datasets, showing that our diffusion-aware D-CoCoA methods achieve a superior performance-efficiency trade-off compared to both standard sampling-based approaches and purely diffusion-specific signals. Our results demonstrate that LLMs do not require a compromise between fast inference and reliable UQ.

## 2 Related Work

UQ for text generation has been extensively studied for autoregressive LLMs. White-box methods leverage internal model signals, aggregating token-level probabilities, predictive entropy, or likelihoods to estimate sequence-level uncertainty (Malinin and Gales, 2021; Fomicheva et al., 2020; Vazhentsev et al., 2025b). Some works suggest training supervised hallucination detectors based on hidden states (Azaria and Mitchell, 2023; Su et al., 2024; Vazhentsev et al., 2025c) or attention maps (Chuang et al., 2024; Vazhentsev et al., 2025a) of LLMs. Black-box UQ methods are usually based on the consistency of generations obtained through repetitive sampling. Approaches such as Semantic Entropy (Kuhn et al., 2023; Farquhar et al., 2024), SAR (Duan et al., 2024), and CoCoA (Vashurin et al., 2025b) combine consistency with probability-based signals.

Recently, diffusion models have emerged as an efficient approach to natural language generation by alleviating the autoregressive decoding bottleneck (Xu et al., 2025; Sahoo et al., 2025, 2026b). Masked diffusion-based models such as LLaDA (Zhu et al., 2025) and Dream (Ye et al., 2025) already demonstrate competitive generation quality with autoregressive counterparts such as LLaMA-3.1 (Grattafiori et al., 2024).

While UQ has been studied for diffusion-based image generation (Jazbec et al., 2025; Kou et al., 2024; Berry et al., 2024), these methods usually do not directly transfer to text generation, where intermediate states are discrete token predictions and semantic meaning is highly non-linear and non-differentiable. A few works leveraged denoising trajectories in LLMs for hallucination detection (Chang et al., 2026; Qian et al., 2026). However, these approaches are strictly supervised and consequently lack the generalization required to seamlessly adapt to new tasks or domains.

In summary, no prior work has introduced a systematic UQ framework for LLDMs. We address this gap by proposing a family of unsupervised methods that explicitly leverage the distinctive properties of the iterative denoising process for UQ. In particular, we show that intermediate denoising trajectories, diffusion statistics, masking dynamics, and denoising complexity can be repurposed into effective and efficient unsupervised uncertainty scores.

### 3 Methodology

#### 3.1 Background

**Generation in LLDMs.** Let  $\mathbf{x}$  denote an input prompt and  $\mathbf{y} = (y_1, \dots, y_{|\mathbf{y}|})$  a generated sequence. Unlike autoregressive LLMs, which generate text sequentially from left to right, LLDMs generate a sequence through an iterative denoising process. Generation starts from a fully corrupted state  $\mathbf{z}_T = (\mathbf{M}, \dots, \mathbf{M})$ , where  $\mathbf{M}$  is a special [MASK] token. The model then gradually reconstructs a clean text sequence by applying a learned reverse denoising process:

$$\mathbf{z}_T \sim q(\mathbf{z}_T), \quad \mathbf{z}_{t-1} \sim p_\theta(\mathbf{z}_{t-1} \mid \mathbf{z}_t, \mathbf{x}), \quad t = T, T-1, \dots, 1.$$

Here,  $\mathbf{z}_t$  denotes the intermediate sequence at step  $t$ ,  $\mathbf{z}_0 = \mathbf{y}$  is the final generated text, and  $p_\theta$  is a neural denoising model parameterized by  $\theta$ . This non-autoregressive inference revises multiple tokens in parallel, making diffusion-based generation faster but conceptually distinct from next-token prediction implemented in standard LLMs.

During training, the model learns to recover the original sequence  $\mathbf{y}$  from a masked corruption  $\mathbf{z}_t$ . A common training objective is a denoising loss:

$$\mathcal{L}(\theta) = -\mathbb{E}_{t, \mathbf{x}, \mathbf{y}, \mathbf{z}_t} \left[ \frac{1}{t} \sum_{i=1}^{|\mathbf{y}|} \mathbf{1}[z_{t,i} = \mathbf{M}] \log p_\theta(y_i \mid \mathbf{z}_t, \mathbf{x}) \right].$$

**UQ methods for hallucination detection** of autoregressive LLMs commonly exploit (1) white-box signals such as token-level probabilities  $p(y_l \mid \mathbf{y}_{<l}, \mathbf{x})$ , aggregated into sequence-level scores, e.g., sequence likelihood  $P(\mathbf{y} \mid \mathbf{x}) = \prod_{l=1}^L p(y_l \mid \mathbf{y}_{<l}, \mathbf{x})$ , and (2) the consistency of sampled generations  $\{\mathbf{y}^{(i)}\}_{i=1}^M, \mathbf{y}^{(i)} \sim p(\mathbf{y} \mid \mathbf{x})$  where uncertainty is computed through lexical and semantic dissimilarity measures between samples (Lin et al., 2024; Zhang et al., 2024; Nikitin et al., 2024). (3) Some methods combine information from sampling with the token probability distributions estimated by LLMs: Monte Carlo Sequence Entropy (Malinin and Gales, 2021), Semantic Entropy (Kuhn et al., 2023; Farquhar et al., 2024), and a recently proposed CoCoA method (Vashurin et al., 2025b). However, two major problems arise when trying to apply these signals to UQ of LLDM generations.

First, LLDMs do not natively use the left-to-right autoregressive factorization of standard LLMs, so token-level probabilities  $p(y_l \mid \mathbf{y}_{<l}, \mathbf{x})$  are not directly available. Moreover, diffusion models generally do not admit an exact tractable likelihood and are instead optimized through a lower-bound objective, making their resulting probabilities unreliable as estimates of sequence likelihood.

Second, sampling multiple generations from LLMs is impractical in general and for LLDMs in particular, as these models are specifically designed for fast and efficient generation (Wu et al., 2026; Sahoo et al., 2026a). Increasing inference cost by a large multiplicative factor through repeated sampling undermines one of their main advantages.

We argue that the iterative denoising process provides additional signals for UQ. For example, the structured trajectory of intermediate states  $\{\mathbf{z}_t\}_{t=1}^T$  reflects how the generation evolves over time and naturally captures variation in the model’s intermediate predictions. We explore these diffusion-specific signals derived from the model’s generation trajectory for UQ in the following section.

#### 3.2 Diffusion-Specific Signals for Uncertainty Quantification

We propose a set of uncertainty scores that directly exploit the denoising generation process, including generation likelihood estimates from LLDM, trajectory statistics, and remasking dynamics.

**Negative log-likelihood estimation.** Nie et al. (2025) propose a Monte Carlo estimator of an upper-bound ELBO-like surrogate for the negative log-likelihood based on the masked diffusion objective. This quantity can serve as an uncertainty score for generated sequences. Let  $N_{mc}$  denote

the number of Monte Carlo samples. For each  $m \in \{1, \dots, N_{mc}\}$ , we obtain  $\mathbf{z}_t$  by sampling  $l_m \sim \text{Uniform}\{1, \dots, |\mathbf{y}|\}$  tokens from  $\mathbf{y}$  without replacement for masking. The Monte Carlo masked negative log-likelihood (MCNLL) estimator is then defined as:

$$\mathbf{u}_{\text{MCNLL}}(\mathbf{x}, \mathbf{y}) = -\frac{1}{N_{mc}} \sum_{m=1}^{N_{mc}} \frac{|\mathbf{y}|}{l_m} \sum_{i=1}^{|\mathbf{y}|} \mathbf{1}[z_{t,i} = \mathbf{M}] \log p_{\theta}(y_i | \mathbf{x}, \mathbf{z}_t). \quad (1)$$

A length-normalized variant,  $\mathbf{u}_{\text{MCNLL}}^{\text{norm}}(\mathbf{x}, \mathbf{y}) = \mathbf{u}_{\text{MCNLL}}(\mathbf{x}, \mathbf{y})/|\mathbf{y}|$ , enables a more consistent comparison across outputs of varying lengths.

**Likelihood-based signals from the denoising trajectory.** Since the denoising process produces a trajectory of intermediate states with probability distributions, it naturally enables UQ via statistics computed along this trajectory. For semi-autoregressive LLDMs,  $\mathbf{y}$  is partitioned into  $B$  blocks of lengths  $L_b$ , and  $B_{\text{valid}}$  denotes the number of non-empty generated blocks (i.e., blocks containing at least one non-special token). We denote  $\tilde{y}_{b,t,k} = \arg \max_{y' \in \mathcal{V}} p_{\theta}(y' | \mathbf{x}, \mathbf{z}_{<b,t,k})$  as the  $k$ -th argmax token over the vocabulary  $\mathcal{V}$  at step  $t$  in block  $b$ , and  $\mathbf{z}_{<b,t,k}$  as the preceding context. Below, we construct several uncertainty scores that take advantage of the diffusion-based trajectory.

(1) The average trajectory negative log-likelihood aggregates the log-probabilities of predicted tokens across the denoising trajectory:

$$\mathbf{u}_{\text{TrajNLL}}(\mathbf{x}, \mathbf{y}) = \frac{1}{B_{\text{valid}} T} \sum_{b,t} \frac{1}{L_b} \sum_{k=1}^{L_b} \log p_{\theta}(\tilde{y}_{b,t,k} | \mathbf{x}, \mathbf{z}_{<b,t,k}). \quad (2)$$

(2) The average predictive entropy captures the average uncertainty of token predictions along the denoising trajectory:

$$\mathbf{u}_{\text{TrajEnt}}(\mathbf{x}, \mathbf{y}) = \frac{1}{B_{\text{valid}} T} \sum_{b,t} \frac{1}{L_b} \sum_{k=1}^{L_b} H(p_{\theta}(\cdot | \mathbf{x}, \mathbf{z}_{<b,t,k})), \quad (3)$$

where  $H(p) = -\sum_{v \in \mathcal{V}} p(v) \log p(v)$  denotes the token-level entropy over the vocabulary  $\mathcal{V}$ .

(3) We further consider the confidence of the model at the moment each token is committed. If tokens are committed with low probability on average, it might indicate high uncertainty. Let  $t_k$  denote the diffusion step at which the  $k$ -th token transitions from a masked to an unmasked (committed) state. The average negative log-likelihood at final commitment across all token positions is:

$$\mathbf{u}_{\text{CommitNLL}}(\mathbf{x}, \mathbf{y}) = -\frac{1}{|\mathbf{y}|} \sum_{b,k} \log p_{\theta}(y_{b,k} | \mathbf{x}, \mathbf{z}_{<b,t_k,k}). \quad (4)$$

**Denoising trajectory-based statistics** also provides useful uncertainty signals.

(1) The Number of Function Evaluations (NFE) denotes the number of LLDM forward passes required to generate an output. While upper-bounded by the maximum number of diffusion steps, NFE is often smaller in practice due to confidence-based remasking and early stopping. It therefore serves as a natural proxy for denoising complexity. Formally, let  $T(\mathbf{y})$  denote the actual NFE used for generating output  $\mathbf{y}$ :

$$\mathbf{u}_{\text{NFE}}(\mathbf{x}, \mathbf{y}) = T(\mathbf{y}). \quad (5)$$

(2) Remasking behavior itself captures instability at the token level. Let  $\mathcal{R}_t$  be the set of tokens remasked at a diffusion step  $t$  during generation; then we consider the average number of masked tokens across all steps:

$$\mathbf{u}_{\text{Remask}}(\mathbf{x}, \mathbf{y}) = \frac{1}{T} \sum_{t=1}^T |\mathcal{R}_t|. \quad (6)$$

(3) Token-level prediction instability is the average number of token flips and consecutive diffusion steps at which the most probable token prediction changes. Frequent prediction changes across steps reflect token-level instability during the denoising process and serve as a proxy for uncertainty. Let  $T_b$  be the number of diffusion steps for the block  $b$ :

$$\mathbf{u}_{\text{FlipCount}}(\mathbf{x}, \mathbf{y}) = \frac{1}{|\mathbf{y}|} \sum_{b,k} \sum_{t=1}^{T_b-1} \mathbf{1}[\tilde{y}_{b,t,k} \neq \tilde{y}_{b,t+1,k}]. \quad (7)$$

**Denoising trajectory semantic instability.** We introduce a novel and highly effective UQ signal that exploits the diffusion-based generation process for zero-shot UQ, avoiding the prohibitive cost of repeated sequence sampling. This signal measures the semantic consistency between intermediate trajectory states and the final generation, capturing the extent of semantic shift before the final output. Accordingly, we define semantic instability across the denoising process via the **average dissimilarity (AD)** between intermediate states  $\tilde{\mathbf{y}}_t$  (obtained via  $\arg \max$  decoding) and the final generation  $\mathbf{y}$ :

$$\mathbf{u}_{\text{AD}}(\mathbf{x}, \mathbf{y}) = \frac{1}{T} \sum_{t=1}^T D(\tilde{\mathbf{y}}_t, \mathbf{y}). \quad (8)$$

Theorem 1 (see below) provides theoretical support for using  $\mathbf{u}_{\text{AD}}$  as a principled uncertainty measure by showing that it lower-bounds the LLDM loss. Consequently, a high value of  $\mathbf{u}_{\text{AD}}$  indicates a high expected prediction error and suggests that the generation is likely to contain hallucinations.

**Theorem 1** (Expected Trajectory Dissimilarity as a Lower Bound on the Masking Loss). *Assume that the model is perfectly calibrated, i.e., Fisher consistency (Nie et al., 2025), meaning it recovers the true posterior:  $p_\theta(\mathbf{y} \mid \mathbf{x}, \mathbf{z}_t) = p_{\text{data}}(\mathbf{y} \mid \mathbf{x}, \mathbf{z}_t)$  almost surely for any masked state  $\mathbf{z}_t$ . Furthermore, assume that the dissimilarity function  $D(\cdot, \cdot)$  acts as an optimal semantic measure, such that  $D(\tilde{\mathbf{y}}_t, \mathbf{y}) = \mathbf{1}[\tilde{\mathbf{y}}_t \neq \mathbf{y}]$ , where the intermediate prediction  $\tilde{\mathbf{y}}_t = \arg \max_{\mathbf{y}'} p_\theta(\mathbf{y}' \mid \mathbf{z}_t, \mathbf{x})$ . Under these assumptions, the expected trajectory dissimilarity is upper-bounded by the masking loss:*

$$\mathbb{E}_{(\mathbf{x}, \mathbf{y}) \sim p_{\text{data}}}[\mathbf{u}_{\text{AD}}(\mathbf{x}, \mathbf{y})] \leq \mathcal{L}(\theta).$$

The proof of Theorem 1 is in Appendix A.1. The assumptions of the theorem are practically well motivated. Perfect calibration, or Fisher consistency, is a standard assumption in diffusion analyses (Nie et al., 2025). Although the semantic measure  $D(\cdot, \cdot)$  is never ideal in practice, its indicator-based definition ensures that any semantic mismatch results in nonzero dissimilarity.

To implement AD, we need to specify how we define the trajectory generation. In practice, generation is semi-autoregressive; therefore, it can be defined in four different ways: (1)  $\tilde{\mathbf{y}}_t^{\text{block}}$ , the trajectory of each block is considered independently; (2)  $\tilde{\mathbf{y}}_t^{\text{last}}$ , we track the trajectory of only the last block, as it usually provides the final answer after CoT thinking; (3)  $\tilde{\mathbf{y}}_t^{\text{last\_prefix}}$ , we fix all blocks  $1..B_{\text{valid}} - 1$  at their final state, and only the last block varies with the prefix of all preceding blocks; (4)  $\tilde{\mathbf{y}}_t^{\text{full}}$ , we consider the whole trajectory of all blocks. We compare these variants in Appendix C.

**Progressive trajectory dissimilarity.** To penalize slow convergence, we apply a progress-based weighting scheme that assigns greater importance to dissimilarities observed at earlier trajectory steps. This reflects the intuition that if the denoising trajectory is already close to the final output within the first few steps, the model stabilizes quickly, indicating low uncertainty. Accordingly, to capture the importance of the early convergence in the beginning of the denoising process while still accounting for later-stage changes in the trajectory, we formulate the progress-weighted score as:

$$\mathbf{u}_{\text{AD}}^{\text{prog}}(\mathbf{x}, \mathbf{y}) = \frac{1}{T} \sum_{t=1}^T w_t D(\tilde{\mathbf{y}}_t, \mathbf{y}), \quad w_t = \frac{t}{T}, \quad t = T, T-1, \dots, 1. \quad (9)$$

**Proposition 1** (Bounds for Progressive Trajectory Dissimilarity). *Assume that  $D(\tilde{\mathbf{y}}_t, \mathbf{y}) \geq 0$  for all  $t$ . Then for any  $(\mathbf{x}, \mathbf{y})$ :*

$$\frac{1}{T} \mathbf{u}_{\text{AD}}(\mathbf{x}, \mathbf{y}) \leq \mathbf{u}_{\text{AD}}^{\text{prog}}(\mathbf{x}, \mathbf{y}) \leq \mathbf{u}_{\text{AD}}(\mathbf{x}, \mathbf{y}). \quad (10)$$

The proof of Proposition 1 is presented in Appendix A.2.

Since  $\mathbf{u}_{\text{AD}}^{\text{prog}}(\mathbf{x}, \mathbf{y}) \leq \mathbf{u}_{\text{AD}}(\mathbf{x}, \mathbf{y})$ , Theorem 1 implies:

$$\mathbb{E}_{(\mathbf{x}, \mathbf{y}) \sim p_{\text{data}}}[\mathbf{u}_{\text{AD}}^{\text{prog}}(\mathbf{x}, \mathbf{y})] \leq \mathbb{E}_{(\mathbf{x}, \mathbf{y}) \sim p_{\text{data}}}[\mathbf{u}_{\text{AD}}(\mathbf{x}, \mathbf{y})] \leq \mathcal{L}(\theta). \quad (11)$$

Therefore, progressive trajectory dissimilarity remains controlled by the masked diffusion reconstruction loss while emphasizing earlier denoising states.

### 3.3 D-CoCoA: Adapting UQ Methods Developed for Autoregressive Generation to LLMs

Diffusion-specific signals address the two major limitations of standard UQ methods for autoregressive generation discussed above. MCNLL provides an upper bound on the sequence negative log-likelihood and can therefore be used in methods that rely on sequence likelihood (Malinin and Gales,

2021; Kuhn et al., 2023; Duan et al., 2024). Intermediate states from the denoising trajectory can replace the set of generations obtained through expensive repeated sampling in consistency-based methods, such as Lexical Similarity (Fomicheva et al., 2020), graph-based methods (Lin et al., 2024), LUQ (Zhang et al., 2024), and KLE (Nikitin et al., 2024). Finally, white-box methods that combine likelihood- and consistency-based components, such as Semantic Entropy (Kuhn et al., 2023), SAR (Duan et al., 2024), Semantic Density (Qiu and Miikkulainen, 2024), and CoCoA (Vashurin et al., 2025b), can benefit from both adaptations.

The latter method, CoCoA, is a state-of-the-art approach in this category. It builds on Minimum Bayes Risk (MBR) estimation and naturally integrates consistency-based signals and information-based scores into a principled confidence estimation framework (Vashurin et al., 2025b). Specifically, it defines a hallucination detection score as a multiplicative combination of self-consistency and information-based uncertainty scores:

$$\mathbf{u}_{\text{CoCoA}}(\mathbf{x}, \mathbf{y}) = \mathbf{u}_{\text{inf}}(\mathbf{x}, \mathbf{y}) \cdot \mathbf{u}_{\text{cons}}(\mathbf{x}, \mathbf{y}). \quad (12)$$

To construct D-CoCoA – a version of this method adapted to LLDMs – we replace the self-consistency component with a trajectory-based semantic dissimilarity AD and the information-based component with one of the diffusion-based scores.

$$\mathbf{u}_{\text{D-CoCoA}}(\mathbf{x}, \mathbf{y}) = \mathbf{u}_{\text{D-inf}}(\mathbf{x}, \mathbf{y}) \cdot \mathbf{u}_{\text{AD}}(\mathbf{x}, \mathbf{y}). \quad (13)$$

Both components can be naturally configured at two levels of granularity, resulting in two versions of the adapted method.

**D-CoCoA Local.** At the token and block level,  $\mathbf{u}_{\text{CommitNLL}}$  provides a natural likelihood proxy unique to LLDMs: it captures model confidence at the precise moment each token is committed, reflecting local generation reliability. Block-level trajectory dissimilarity isolates semantic instability within each generation block independently, which yields:

$$\mathbf{u}_{\text{D-CoCoA-L}}(\mathbf{x}, \mathbf{y}) = \mathbf{u}_{\text{CommitNLL}}(\mathbf{x}, \mathbf{y}) \cdot \mathbf{u}_{\text{AD-Block}}(\mathbf{x}, \mathbf{y}). \quad (14)$$

**D-CoCoA Global.**  $\mathbf{u}_{\text{MCNLL}}$  admits a principled approximation of the likelihood over the entire output. Full trajectory dissimilarity measures global semantic drift across all blocks. This global view naturally extends with NFE as a diffusion-specific complexity penalty, yielding:

$$\mathbf{u}_{\text{D-CoCoA-G}}(\mathbf{x}, \mathbf{y}) = \mathbf{u}_{\text{MCNLL}}^{\text{norm}}(\mathbf{x}, \mathbf{y}) \cdot (\mathbf{u}_{\text{NFE}}(\mathbf{x}, \mathbf{y}) \cdot \mathbf{u}_{\text{AD-Full}}(\mathbf{x}, \mathbf{y})). \quad (15)$$

## 4 Experiments

### 4.1 Experimental Setup

We evaluate the effectiveness of UQ methods in identifying and filtering unreliable model outputs under a selective generation setting (Vashurin et al., 2025a). Implementation details of the experimental setup are presented in Appendix D.1.

**Datasets.** We evaluate UQ methods on eight benchmarks spanning question answering (MMLU, TriviaQA, CoQA, GSM8k), summarization (SamSum, XSum), and machine translation (WMT14 fr→en, WMT19 de→en). Detailed dataset characteristics, prompts, and generation hyperparameters are reported in Appendix D.3.

**Models.** We conduct all experiments using LLaDA-1.5 (Zhu et al., 2025) and Dream (Ye et al., 2025), instruction-tuned 7B-parameter masked LLDMs.

**UQ baselines.** We evaluate all proposed and adapted diffusion-specific UQ methods in Section 3 against state-of-the-art classical likelihood-based, sampling-based, and supervised baselines developed for autoregressive generation, enabling a comprehensive comparison across paradigms. Full details of all UQ baseline methods for autoregressive generation are provided in Appendix D.2.

**Evaluation metrics.** UQ performance is primarily measured using the Prediction Rejection Ratio (PRR) – a standard metric for benchmarking UQ methods in selective classification and generation (Malinin and Gales, 2021; Vashurin et al., 2025a). PRR summarizes the area under the rejection curve, which shows the average quality of the retained responses after abstaining from a given fraction of the most uncertain predictions. The metric is normalized and typically falls within a [0,

UQ Method	XSum	SamSum	WMT14	WMT19	CoQA	TriviaQA	MMLU	GSM8k	Mean
MSP	-0.07	0.11	0.20	0.16	-0.02	0.05	0.34	0.09	0.11
MTE	-0.01	0.02	0.34	0.30	0.06	0.02	0.34	0.10	0.15
Perplexity	-0.09	0.03	0.21	0.17	-0.02	0.04	0.34	0.04	0.09
AttScore	0.29	0.17	0.07	0.03	0.04	0.09	0.05	0.18	0.11
CCP	-0.10	0.10	0.19	0.12	-0.03	0.05	0.34	0.08	0.09
RAUQ	-0.04	0.08	0.26	0.20	0.00	0.05	0.34	0.12	0.13
MCNSE	-0.07	0.07	0.29	0.25	-0.00	0.08	0.30	0.06	0.12
SemanticEntropy	-0.04	0.15	0.35	0.36	0.04	0.11	0.42	0.13	0.19
SAR	0.07	0.21	0.43	0.46	0.20	0.46	0.42	0.16	0.30
EigenScore	0.14	0.15	0.49	0.49	0.20	0.44	0.39	0.45	0.34
CoCoA-MTE	0.09	0.18	0.51	0.53	0.17	0.26	0.43	0.20	0.30
SemanticDensity	0.21	0.27	0.42	0.45	0.09	0.44	0.11	0.08	0.26
LUQ	0.22	0.20	0.43	0.45	0.30	0.60	0.43	0.19	0.35
KLE	0.22	0.24	0.44	0.48	0.27	0.60	0.43	0.17	0.36
DegMat	0.21	0.19	0.43	0.48	0.25	0.59	0.43	0.16	0.34
SAPLMA	0.29	0.32	0.57	0.59	0.04	0.56	0.23	0.31	0.36
SATRMD	0.14	0.12	0.32	0.23	0.08	0.31	0.26	0.06	0.19
LookBackLens	0.29	-0.09	0.54	0.53	0.19	0.51	0.02	0.21	0.27
TAD	0.20	0.38	0.54	0.51	0.14	0.51	0.34	0.35	0.37

Table 1: PRR $\uparrow$  for the LLaDa 7b v1.5 model for various tasks for the considered classical autoregressive methods (see Tab. 7 for the Dream model). Warmer color indicates better results.

1] range: 0 corresponds to random rejection, whereas 1 corresponds to the optimal rejection order. Compared to ROC-AUC, PRR is less sensitive to class imbalance, supports continuous generation-quality metrics, and can be naturally evaluated at practically relevant rejection rates. We compute PRR for rejection rates of up to 50% (over only the first part of the curve), as rejecting more than half of the instances is typically impractical. We evaluate PRR using task-specific generation quality measures: accuracy for MMLU and GSM8k; COMET (Rei et al., 2020) for MT; and AlignScore (Zha et al., 2023) for the rest. We additionally report results with the ROC-AUC metric in Appendix B.3.

Since LLDMs target efficient generation, we also assess computational overhead. We define overhead as the extra runtime beyond base generation, including auxiliary model calls (e.g., the Cross-Encoder required by CoCoA).

## 4.2 Analysis of Baselines

**UQ methods designed for autoregressive generation.** We first evaluate common UQ methods designed for autoregressive LLMs (Table 1 for LLaDa; Table 7 in Appendix B.2 for Dream).

First, *information-based methods that rely solely on the logits or attention maps perform poorly*, typically only marginally better than random. This is the result of the mismatch between the generation process and the probability estimates used in these methods.

Second, because information-based scores are poorly aligned with LLDMs, white-box sampling-based methods that rely on these scores also do not perform well and are generally outperformed by black-box sampling-based methods, which depend only on the consistency of the generated texts. Overall, *black-box methods achieve the strongest performance among the UQ methods originally designed for autoregressive generation*, with KLE standing out as the best-performing method.

Third, *supervised methods that rely on engineered features derived from the model’s internal states, such as SATRMD and LookBackLens, typically perform poorly for LLDMs*. This further illustrates that the inductive biases underlying feature-engineering approaches designed for autoregressive LLMs are not well aligned with diffusion-style generation. Other supervised methods that use raw LLM internal states without complex engineering, such as SAPLMA and TAD, perform substantially better but still fail to outperform black-box sampling-based methods. This is surprising since supervised UQ methods are typically among the strongest approaches for in-domain evaluations.

**Diffusion-specific UQ methods: MCNLL, and likelihood- and statistics-based signals from the denoising trajectory.** Tables 2 and 8 in Appendix B.2 show results with diffusion-specific methods for LLaDa and Dream, respectively. *All considered statistics typically provide useful information*, except NFE and RemaskCount on MMLU due to one-step generation. Other methods perform similarly on average.

**Methods based on denoising trajectory semantics instability.** Table 3 and 9 in Appendix B.2 present the results of methods based on the semantic instability of the denoising trajectory during the generation process for LLaDa and Dream, respectively. The performance on MMLU is close to

UQ Method	XSum	SamSum	WMT14	WMT19	CoQA	TriviaQA	MMLU	GSM8k	Mean
MCNLL	0.17	0.18	0.29	0.32	0.24	0.31	0.35	0.23	0.26
MCNLL-Norm	0.17	0.09	0.19	0.24	0.18	0.09	0.35	-0.02	0.16
NFE	0.15	0.17	0.31	0.31	0.22	0.18	0.02	0.29	0.21
Remask	0.16	0.17	0.24	0.26	0.25	0.15	0.02	0.29	0.19
FlipCount	0.15	0.16	0.19	0.19	0.25	0.12	0.02	0.27	0.17
TrajNLL	0.17	0.17	0.20	0.24	0.30	0.25	0.47	0.18	0.25
TrajEntropy	0.16	0.20	0.26	0.30	0.28	0.29	0.47	0.22	0.27
CommitNLL	0.18	0.19	0.39	0.43	0.22	0.43	0.47	0.30	0.33

Table 2: PRR $\uparrow$  for the LLaDA-7B-v1.5 model for various diffusion-specific UQ baselines (see Tab. 8 for the Dream model). Darker color indicates better results.

UQ Method	XSum	SamSum	WMT14	WMT19	CoQA	TriviaQA	MMLU	GSM8k	Mean
AD-Block	0.19	0.05	0.15	0.32	0.23	0.39	-0.05	-0.15	0.14
WeightedAD-Block	0.20	0.18	0.27	0.38	0.26	0.39	-0.05	0.22	0.23
AD-LastBlock	0.16	0.10	0.21	0.34	0.23	0.39	-0.05	0.06	0.18
WeightedAD-LastBlock	0.15	0.12	0.27	0.38	0.26	0.39	-0.05	0.07	0.20
AD-LastBlockPrefix	0.15	0.19	0.18	0.32	0.29	0.39	-0.05	0.01	0.18
WeightedAD-LastBlockPrefix	0.16	0.17	0.24	0.36	0.32	0.39	-0.05	0.03	0.20
AD-Full	0.09	0.22	0.25	0.36	0.29	0.39	-0.05	0.03	0.20
WeightedAD-Full	0.09	0.21	0.28	0.38	0.32	0.39	-0.05	0.04	0.21

Table 3: PRR $\uparrow$  for the LLaDA-7B-v1.5 model for various trajectory dissimilarity baselines (see Tab. 9 for the Dream model). Darker color indicates better results.

random because the trajectories contain only one step. For TriviaQA, all results are similar because there is only one block across all outputs. The weighted version typically outperforms the original average dissimilarity. Furthermore, all block-wise trajectory evaluations are generally worse than the raw full trajectory without any specific aggregation across all datasets, except for GSM8k. Overall, results show that *average trajectory dissimilarity proves to be a highly informative signal*.

**White-box sampling-based UQ with MCNLL for likelihood estimation.** Table 4 and 10 in Appendix B present the results with sampling-based baselines for standard autoregressive LLMs, where the generated sequence likelihood is estimated using MCNLL for LLaDa and Dream, respectively. As expected, *MCNLL consistently and substantially improves performance across all methods and datasets*. CoCoA-MCNLL achieves the best average results across all considered methods, outperforming the best non-diffusion-specific method, KLE, for the LLaDa model.

**Black-box sampling-based UQ with denoising trajectory states.** Table 5 and 11 in Appendix B report results for sampling-based baselines adapted to use intermediate generations from the denoising trajectory instead of independently sampled outputs. Most adapted methods, except D-KLE, yield meaningful uncertainty estimates, but they substantially underperform AD. Since both approaches rely only on the denoising trajectory, this comparison highlights the importance of the right aggregation: D-DegMat, D-KLE, and related methods compute pairwise similarities among trajectory states, whereas AD measures the dissimilarity between each intermediate state and the final output.

**Summary.** This analysis yields three main findings: (1) UQ methods based on generation likelihood should use the diffusion-aware likelihood estimation, such as MCNLL; (2) denoising trajectory statistics provide useful uncertainty signals; and (3) intermediate states in the denoising process can be used instead of sampling multiple final generations, with the strongest UQ signal obtained by measuring their dissimilarity to the final generation.

### 4.3 Main Results

Having established the behavior of individual categories of methods, we now compare the best methods under a unified performance-efficiency framework. Figure 2 presents the trade-off between selective generation performance (measured by PRR) and computational complexity (measured as overhead time) averaged across all datasets. Figures 3 and 4 in Appendix B present the detailed trade-off between selective generation performance and computational complexity for all individual datasets. The detailed PRR scores are presented in Tables 6 and 12 in Appendix B.

Overall, we observe a clear efficiency-performance frontier. Extensive sampling methods, such as basic CoCoA variants, DegMat, and SAR, achieve higher PRR but incur substantially greater computational overhead. In contrast, lightweight diffusion-specific signals, such as NFE and trajectory-

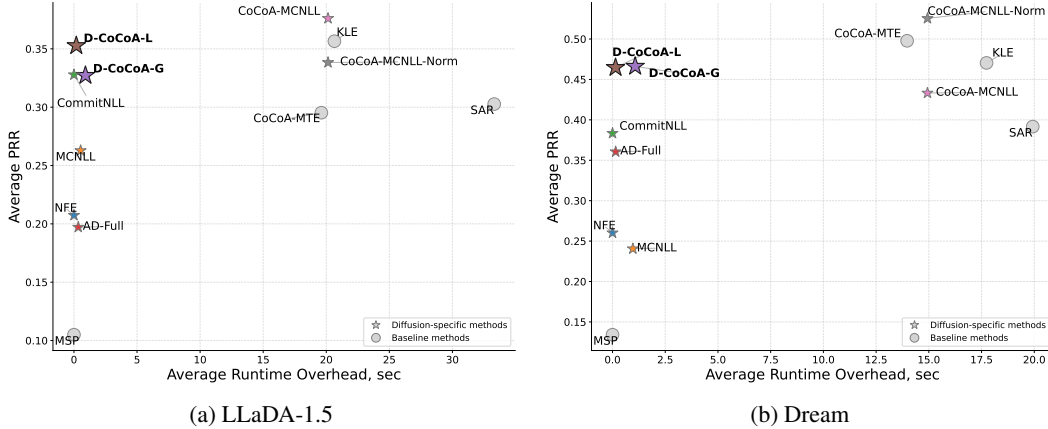


Figure 2: UQ performance (PRR $\uparrow$ ) versus computational overhead (runtime in seconds $\downarrow$ ) averaged across all datasets.

based statistics, provide very low-cost uncertainty estimates but are less accurate and generally insufficient for high-quality UQ.

Our proposed methods, D-CoCoA-G and D-CoCoA-L, consistently achieve a strong balance between performance and efficiency. They clearly outperform other low- to medium-complexity methods and approach the performance of substantially more expensive sampling-based methods. This trade-off is highly favorable: for example, D-CoCoA-L requires roughly **one hundred times less** additional computation time than the best-performing methods, CoCoA-MCNLL and KLE, while these methods provide only modest additional gains (e.g. 2.4% for LLaDA). This trend holds both on average and across individual datasets.

**Key take-away:** Experimental results show that by leveraging the distinctive properties of the LLDMs denoising process, we can obtain strong uncertainty estimates at almost no additional cost while preserving computational efficiency – one of the main motivations for using LLDMs.

**Ablation summary.** We ablate four D-CoCoA components: source of likelihood, trajectory aggregation strategy, similarity function, and the optional NFE term. We find that the default configuration (MCNLL likelihood, full trajectory for D-CoCoA-G and per-block averaging for D-CoCoA-L, RoBERTa Cross-Encoder similarity) yields the best average performance; including NFE further benefits D-CoCoA-G but slightly hurts D-CoCoA-L. The full ablation tables and per-component discussion are reported in Appendix C.

## 5 Conclusion

We presented the first systematic study of unsupervised UQ for LLDMs. We showed that UQ methods developed for autoregressive LLMs are often poorly aligned with diffusion-based generation, either because they rely on left-to-right sequence likelihoods or because they require repeated sampling that undermines the efficiency advantages of LLDMs. To address this gap, we introduced a family of diffusion-specific uncertainty signals derived directly from the denoising process, including masked diffusion likelihoods, trajectory statistics, remasking dynamics, generation complexity, and semantic instability along the denoising trajectory.

Building on these signals, we proposed D-CoCoA, a diffusion-aware adaptation of a state-of-the-art hybrid UQ method. Our theoretical analysis connects trajectory dissimilarity to the masked diffusion training objective, providing support for its use as a principled uncertainty measure. Our experiments show that D-CoCoA achieves a favorable performance-efficiency trade-off: it approaches or matches strong sampling-based baselines while requiring substantially lower computational overhead. Overall, our results demonstrate that LLDMs can support reliable hallucination detection without sacrificing their core advantage of fast inference.

## References

- A. Azaria and T. Mitchell. The internal state of an LLM knows when it’s lying. In H. Bouamor, J. Pino, and K. Bali, editors, *Findings of the Association for Computational Linguistics: EMNLP 2023*, pages 967–976, Singapore, Dec. 2023. Association for Computational Linguistics.
- L. Barrault, O. Bojar, M. R. Costa-jussà, C. Federmann, M. Fishel, Y. Graham, B. Haddow, M. Huck, P. Koehn, S. Malmasi, C. Monz, M. Müller, S. Pal, M. Post, and M. Zampieri. Findings of the 2019 Conference on Machine Translation (WMT19). In O. Bojar, R. Chatterjee, C. Federmann, M. Fishel, Y. Graham, B. Haddow, M. Huck, A. J. Yepes, P. Koehn, A. Martins, C. Monz, M. Negri, A. Névól, M. Neves, M. Post, M. Turchi, and K. Verspoor, editors, *Proceedings of the Fourth Conference on Machine Translation (Volume 2: Shared Task Papers, Day 1)*, pages 1–61, Florence, Italy, Aug. 2019. Association for Computational Linguistics.
- L. Berry, A. Brando, and D. Meger. Shedding light on large generative networks: Estimating epistemic uncertainty in diffusion models. In N. Kiyavash and J. M. Mooij, editors, *Uncertainty in Artificial Intelligence, 15-19 July 2024, Universitat Pompeu Fabra, Barcelona, Spain*, Proceedings of Machine Learning Research, pages 360–376. PMLR, 2024.
- T. Bie, M. Cao, K. Chen, L. Du, M. Gong, Z. Gong, Y. Gu, J. Hu, Z. Huang, Z. Lan, C. Li, C. Li, J. Li, Z. Li, H. Liu, L. Liu, G. Lu, X. Lu, Y. Ma, J. Tan, L. Wei, J. Wen, Y. Xing, X. Zhang, J. Zhao, D. Zheng, J. Zhou, J. Zhou, Z. Zhou, L. Zhu, and Y. Zhuang. LLaDA2.0: Scaling up diffusion language models to 100b. *CoRR*, abs/2512.15745, 2025.
- O. Bojar, C. Buck, C. Federmann, B. Haddow, P. Koehn, J. Leveling, C. Monz, P. Pecina, M. Post, H. Saint-Amand, R. Soricut, L. Specia, and A. Tamchyna. Findings of the 2014 workshop on statistical machine translation. In O. Bojar, C. Buck, C. Federmann, B. Haddow, P. Koehn, C. Monz, M. Post, and L. Specia, editors, *Proceedings of the Ninth Workshop on Statistical Machine Translation*, pages 12–58, Baltimore, Maryland, USA, June 2014. Association for Computational Linguistics.
- S. Chang, J. Yu, W. Wang, Y. Chen, J. Yu, P. Torr, and J. Gu. TRACEDET: Hallucination Detection From the Decoding Trace of Diffusion Large Language Models. In *The Fourteenth International Conference on Learning Representations*, 2026.
- C. Chen, K. Liu, Z. Chen, Y. Gu, Y. Wu, M. Tao, Z. Fu, and J. Ye. INSIDE: LLMs’ internal states retain the power of hallucination detection. In *The Twelfth International Conference on Learning Representations*, 2024.
- Y.-S. Chuang, L. Qiu, C.-Y. Hsieh, R. Krishna, Y. Kim, and J. R. Glass. Lookback lens: Detecting and mitigating contextual hallucinations in large language models using only attention maps. In Y. Al-Onaizan, M. Bansal, and Y.-N. Chen, editors, *Proceedings of the 2024 Conference on Empirical Methods in Natural Language Processing*, pages 1419–1436, Miami, Florida, USA, Nov. 2024. Association for Computational Linguistics.
- K. Cobbe, V. Kosaraju, M. Bavarian, M. Chen, H. Jun, L. Kaiser, M. Plappert, J. Tworek, J. Hilton, R. Nakano, C. Hesse, and J. Schulman. Training verifiers to solve math word problems. *CoRR*, abs/2110.14168, 2021.
- J. Duan, H. Cheng, S. Wang, A. Zavalny, C. Wang, R. Xu, B. Kailkhura, and K. Xu. Shifting attention to relevance: Towards the predictive uncertainty quantification of free-form large language models. In L.-W. Ku, A. Martins, and V. Srikumar, editors, *Proceedings of the 62nd Annual Meeting of the Association for Computational Linguistics (Volume 1: Long Papers)*, pages 5050–5063, Bangkok, Thailand, Aug. 2024. Association for Computational Linguistics.
- E. Fadeeva, R. Vashurin, A. Tsvigun, A. Vazhentsev, S. Petrakov, K. Fedyanin, D. Vasilev, E. Goncharova, A. Panchenko, M. Panov, T. Baldwin, and A. Shelmanov. LM-polygraph: Uncertainty estimation for language models. In Y. Feng and E. Lefever, editors, *Proceedings of the 2023 Conference on Empirical Methods in Natural Language Processing: System Demonstrations*, pages 446–461, Singapore, Dec. 2023. Association for Computational Linguistics.

- E. Fadeeva, A. Rubashevskii, A. Shelmanov, S. Petrakov, H. Li, H. Mubarak, E. Tsymbalov, G. Kuzmin, A. Panchenko, T. Baldwin, P. Nakov, and M. Panov. Fact-checking the output of large language models via token-level uncertainty quantification. In L.-W. Ku, A. Martins, and V. Srikumar, editors, *Findings of the Association for Computational Linguistics: ACL 2024*, pages 9367–9385, Bangkok, Thailand, Aug. 2024. Association for Computational Linguistics.
- S. Farquhar, J. Kossen, L. Kuhn, and Y. Gal. Detecting hallucinations in large language models using semantic entropy. *Nature*, 630(8017):625–630, 2024.
- M. Fomicheva, S. Sun, L. Yankovskaya, F. Blain, F. Guzmán, M. Fishel, N. Aletras, V. Chaudhary, and L. Specia. Unsupervised quality estimation for neural machine translation. *Transactions of the Association for Computational Linguistics*, 8:539–555, 2020.
- B. Gliwa, I. Mochol, M. Biesek, and A. Wawer. SAMSum corpus: A human-annotated dialogue dataset for abstractive summarization. In L. Wang, J. C. K. Cheung, G. Carenini, and F. Liu, editors, *Proceedings of the 2nd Workshop on New Frontiers in Summarization*, pages 70–79, Hong Kong, China, Nov. 2019. Association for Computational Linguistics.
- A. Grattafiori, A. Dubey, A. Jauhri, A. Pandey, A. Kadian, A. Al-Dahle, A. Letman, A. Mathur, A. Schelten, A. Vaughan, A. Yang, A. Fan, A. Goyal, et al. The Llama 3 herd of models. *arXiv preprint arXiv:2407.21783*, 2024.
- D. Hendrycks, C. Burns, S. Basart, A. Zou, M. Mazeika, D. Song, and J. Steinhardt. Measuring massive multitask language understanding. In *9th International Conference on Learning Representations, ICLR 2021, Virtual Event, Austria, May 3-7, 2021*. OpenReview.net, 2021.
- L. Huang, W. Yu, W. Ma, W. Zhong, Z. Feng, H. Wang, Q. Chen, W. Peng, X. Feng, B. Qin, et al. A survey on hallucination in large language models: Principles, taxonomy, challenges, and open questions. *ACM Transactions on Information Systems*, 43(2):1–55, 2025.
- M. Jazbec, E. Wong-Toi, G. Xia, D. Zhang, E. T. Nalisnick, and S. Mandt. Generative uncertainty in diffusion models. In S. Chiappa and S. Magliacane, editors, *Conference on Uncertainty in Artificial Intelligence, Rio Othon Palace, Rio de Janeiro, Brazil, 21-25 July 2025*, Proceedings of Machine Learning Research, pages 1837–1858. PMLR, 2025.
- M. Joshi, E. Choi, D. Weld, and L. Zettlemoyer. TriviaQA: A large scale distantly supervised challenge dataset for reading comprehension. In R. Barzilay and M.-Y. Kan, editors, *Proceedings of the 55th Annual Meeting of the Association for Computational Linguistics (Volume 1: Long Papers)*, pages 1601–1611, Vancouver, Canada, July 2017. Association for Computational Linguistics.
- S. Kou, L. Gan, D. Wang, C. Li, and Z. Deng. Bayesdiff: Estimating pixel-wise uncertainty in diffusion via bayesian inference. In *The Twelfth International Conference on Learning Representations*, 2024.
- L. Kuhn, Y. Gal, and S. Farquhar. Semantic uncertainty: Linguistic invariances for uncertainty estimation in natural language generation. In *The Eleventh International Conference on Learning Representations, ICLR 2023, Kigali, Rwanda, May 1-5, 2023*. OpenReview.net, 2023.
- Z. Lin, S. Trivedi, and J. Sun. Generating with confidence: Uncertainty quantification for black-box large language models. *Transactions on Machine Learning Research*, 2024. ISSN 2835-8856.
- A. Malinin and M. J. F. Gales. Uncertainty estimation in autoregressive structured prediction. In *9th International Conference on Learning Representations, ICLR 2021, Virtual Event, Austria, May 3-7, 2021*. OpenReview.net, 2021.
- S. Narayan, S. B. Cohen, and M. Lapata. Don’t give me the details, just the summary! topic-aware convolutional neural networks for extreme summarization. In E. Riloff, D. Chiang, J. Hockenmaier, and J. Tsujii, editors, *Proceedings of the 2018 Conference on Empirical Methods in Natural Language Processing*, pages 1797–1807, Brussels, Belgium, Oct.-Nov. 2018. Association for Computational Linguistics.
- S. Nie, F. Zhu, Z. You, X. Zhang, J. Ou, J. Hu, J. Zhou, Y. Lin, J.-R. Wen, and C. Li. Large language diffusion models. In *Advances in Neural Information Processing Systems*, volume 38, 2025.

- A. Nikitin, J. Kossen, Y. Gal, and P. Marttinen. Kernel language entropy: Fine-grained uncertainty quantification for LLMs from semantic similarities. In *Advances in Neural Information Processing Systems*, volume 37, pages 8901–8929, 2024.
- Y. Qian, Y. Tan, Y. Liu, W. Yu, and S. Pan. DynHD: Hallucination detection for diffusion large language models via denoising dynamics deviation learning. *arXiv preprint arXiv:2603.16459*, 2026.
- X. Qiu and R. Miikkulainen. Semantic density: Uncertainty quantification for large language models through confidence measurement in semantic space. In A. Globerson, L. Mackey, D. Belgrave, A. Fan, U. Paquet, J. Tomczak, and C. Zhang, editors, *Advances in Neural Information Processing Systems*, volume 37, pages 134507–134533. Curran Associates, Inc., 2024.
- S. Reddy, D. Chen, and C. D. Manning. CoQA: A conversational question answering challenge. *Transactions of the Association for Computational Linguistics*, 7:249–266, 2019.
- R. Rei, C. Stewart, A. C. Farinha, and A. Lavie. COMET: A neural framework for MT evaluation. In B. Webber, T. Cohn, Y. He, and Y. Liu, editors, *Proceedings of the 2020 Conference on Empirical Methods in Natural Language Processing (EMNLP)*, pages 2685–2702, Online, Nov. 2020. Association for Computational Linguistics.
- S. S. Sahoo, M. Arriola, Y. Schiff, A. Gokaslan, E. Marroquin, J. T. Chiu, A. Rush, and V. Kuleshov. Simple and effective masked diffusion language models. In *Advances in Neural Information Processing Systems*, volume 37, pages 130136–130184, 2024.
- S. S. Sahoo, J. Deschenaux, A. Gokaslan, G. Wang, J. T. Chiu, and V. Kuleshov. The diffusion duality. In *Proceedings of the 42nd International Conference on Machine Learning*, volume 267 of *Proceedings of Machine Learning Research*, pages 52584–52619. PMLR, 2025.
- S. S. Sahoo, J. Lemercier, Z. Yang, J. Deschenaux, J. Liu, J. Thickstun, and A. Jukic. Scaling beyond masked diffusion language models. *CoRR*, abs/2602.15014, 2026a.
- S. S. Sahoo, Z. Yang, Y. Akhauri, J. Liu, D. Singh, Z. Cheng, Z. Liu, E. P. Xing, J. Thickstun, and A. Vahdat. Esoteric language models: Bridging autoregressive and masked diffusion LLMs. In *ICLR 2026 Workshop on Multimodal Intelligence*, 2026b.
- G. Sriramanan, S. Bharti, V. S. Sadasivan, S. Saha, P. Kattakinda, and S. Feizi. LLM-check: Investigating detection of hallucinations in large language models. In A. Globerson, L. Mackey, D. Belgrave, A. Fan, U. Paquet, J. Tomczak, and C. Zhang, editors, *Advances in Neural Information Processing Systems*, volume 37, pages 34188–34216. Curran Associates, Inc., 2024.
- W. Su, C. Wang, Q. Ai, Y. Hu, Z. Wu, Y. Zhou, and Y. Liu. Unsupervised real-time hallucination detection based on the internal states of large language models. In L.-W. Ku, A. Martins, and V. Srikumar, editors, *Findings of the Association for Computational Linguistics: ACL 2024*, pages 14379–14391, Bangkok, Thailand, Aug. 2024. Association for Computational Linguistics.
- R. Vashurin, E. Fadeeva, A. Vazhentsev, L. Rvanova, D. Vasilev, A. Tsvigun, S. Petrakov, R. Xing, A. Sadallah, K. Grishchenkov, A. Panchenko, T. Baldwin, P. Nakov, M. Panov, and A. Shelmanov. Benchmarking uncertainty quantification methods for large language models with LM-polygraph. *Transactions of the Association for Computational Linguistics*, 13:220–248, 2025a.
- R. Vashurin, M. Goloburda, A. Ilina, A. Rubashevskii, P. Nakov, A. Shelmanov, and M. Panov. CoCoA: A minimum bayes risk framework bridging confidence and consistency for uncertainty quantification in LLMs. In *Advances in Neural Information Processing Systems*, volume 38, 2025b.
- A. Vazhentsev, E. Fadeeva, R. Xing, G. Kuzmin, I. Lazichny, A. Panchenko, P. Nakov, T. Baldwin, M. Panov, and A. Shelmanov. Unconditional truthfulness: Learning unconditional uncertainty of large language models. In C. Christodoulopoulos, T. Chakraborty, C. Rose, and V. Peng, editors, *Proceedings of the 2025 Conference on Empirical Methods in Natural Language Processing*, pages 35673–35694, Suzhou, China, Nov. 2025a. Association for Computational Linguistics. ISBN 979-8-89176-332-6.

- A. Vazhentsev, L. Rvanova, G. Kuzmin, E. Fadeeva, I. Lazichny, A. Panchenko, M. Panov, T. Baldwin, M. Sachan, P. Nakov, and A. Shelmanov. Uncertainty-aware attention heads: Efficient unsupervised uncertainty quantification for LLMs. *CoRR*, abs/2505.20045, 2025b.
- A. Vazhentsev, L. Rvanova, I. Lazichny, A. Panchenko, M. Panov, T. Baldwin, and A. Shelmanov. Token-level density-based uncertainty quantification methods for eliciting truthfulness of large language models. In L. Chiruzzo, A. Ritter, and L. Wang, editors, *Proceedings of the 2025 Conference of the Nations of the Americas Chapter of the Association for Computational Linguistics: Human Language Technologies (Volume 1: Long Papers)*, pages 2246–2262, Albuquerque, New Mexico, Apr. 2025c. Association for Computational Linguistics. ISBN 979-8-89176-189-6.
- C. Wu, H. Zhang, S. Xue, Z. Liu, S. Diao, L. Zhu, P. Luo, S. Han, and E. Xie. Fast-dLLM: Training-free acceleration of diffusion LLM by enabling KV cache and parallel decoding. In *The Fourteenth International Conference on Learning Representations*, 2026.
- M. Xu, T. Geffner, K. Kreis, W. Nie, Y. Xu, J. Leskovec, S. Ermon, and A. Vahdat. Energy-based diffusion language models for text generation. In *The Thirteenth International Conference on Learning Representations, ICLR 2025, Singapore, April 24-28, 2025*. OpenReview.net, 2025.
- J. Ye, Z. Xie, L. Zheng, J. Gao, Z. Wu, X. Jiang, Z. Li, and L. Kong. Dream 7B: Diffusion large language models. *arXiv preprint arXiv:2508.15487*, 2025.
- Y. Zha, Y. Yang, R. Li, and Z. Hu. AlignScore: Evaluating factual consistency with a unified alignment function. In A. Rogers, J. Boyd-Graber, and N. Okazaki, editors, *Proceedings of the 61st Annual Meeting of the Association for Computational Linguistics (Volume 1: Long Papers)*, pages 11328–11348, Toronto, Canada, July 2023. Association for Computational Linguistics.
- C. Zhang, F. Liu, M. Basaldella, and N. Collier. LUQ: Long-text uncertainty quantification for LLMs. In Y. Al-Onaizan, M. Bansal, and Y.-N. Chen, editors, *Proceedings of the 2024 Conference on Empirical Methods in Natural Language Processing*, pages 5244–5262, Miami, Florida, USA, Nov. 2024. Association for Computational Linguistics.
- F. Zhu, R. Wang, S. Nie, X. Zhang, C. Wu, J. Hu, J. Zhou, J. Chen, Y. Lin, J.-R. Wen, and C. Li. LLaDA 1.5: Variance-reduced preference optimization for large language diffusion models. *arXiv preprint arXiv:2505.19223*, 2025.

## A Proofs

### A.1 Proof of Theorem 1

Let  $\mathbf{z}_t$  denote the sequence  $\mathbf{y}$  where each token is independently replaced by the [MASK] token with probability  $t \in (0, 1]$ . Let  $\mathcal{M}_t$  be the set of masked positions, such that  $\mathbb{E}[|\mathcal{M}_t|] = t|\mathbf{y}|$ . The full masking loss is  $\mathcal{L}(\theta)$ . Let the reverse process be uniformly discretized into  $T$  steps. In this case we discretization of loss  $\mathcal{L}^{\text{discr.}}(\theta) = \frac{1}{T} \sum_{t=1}^T \mathcal{L}_t^{\text{discr.}}(\theta)$  where:

$$\mathcal{L}_t^{\text{discr.}}(\theta) = \mathbb{E}_{\mathbf{y}, \mathbf{z}_t, \mathbf{x}} \left[ \frac{T}{t} \sum_{i \in \mathcal{M}_t} -\log p_\theta(y_i | \mathbf{z}_t, \mathbf{x}) \right]. \quad (16)$$

Also, we have the property that  $\lim_{T \rightarrow \infty} \mathcal{L}^{\text{discr.}}(\theta) = \mathcal{L}(\theta)$  (Sahoo et al., 2024).

The trajectory dissimilarity metric is defined as  $\mathbf{u}_{\text{AD}}(\mathbf{x}, \mathbf{y}) = \frac{1}{T} \sum_{t=1}^T \mathbf{1}[\tilde{\mathbf{y}}_t \neq \mathbf{y}]$ . By linearity of expectation,

$$\mathbb{E}_{(\mathbf{x}, \mathbf{y}) \sim p_{\text{data}}} [\mathbf{u}_{\text{AD}}(\mathbf{x}, \mathbf{y})] = \frac{1}{T} \sum_{t=1}^T \mathbb{E}_{(\mathbf{x}, \mathbf{y}) \sim p_{\text{data}}} [\mathbf{1}[\tilde{\mathbf{y}}_t \neq \mathbf{y}]] = \frac{1}{T} \sum_{t=1}^T \mathbb{P}(\tilde{\mathbf{y}}_t \neq \mathbf{y}). \quad (17)$$

Conditioning on  $(\mathbf{z}_t, \mathbf{x})$  and using the calibration assumption,  $\mathbb{P}(\tilde{\mathbf{y}}_t \neq \mathbf{y} | \mathbf{z}_t, \mathbf{x}) = 1 - p_\theta(\tilde{\mathbf{y}}_t | \mathbf{z}_t, \mathbf{x})$ . Marginalizing over  $(\mathbf{z}_t, \mathbf{x})$ , we obtain:

$$\mathbb{P}(\tilde{\mathbf{y}}_t \neq \mathbf{y}) = \mathbb{E}_{(\mathbf{z}_t, \mathbf{x})} [1 - p_\theta(\tilde{\mathbf{y}}_t | \mathbf{z}_t, \mathbf{x})]. \quad (18)$$

Since  $\tilde{\mathbf{y}}_t = \arg \max_{\mathbf{y}'} p_\theta(\mathbf{y}' | \mathbf{z}_t, \mathbf{x})$ , we have  $p_\theta(\tilde{\mathbf{y}}_t | \mathbf{z}_t, \mathbf{x}) \geq p_\theta(\mathbf{y}' | \mathbf{z}_t, \mathbf{x})$  for any  $\mathbf{y}'$ . Thus, employing the standard inequality  $1 - p \leq -\log p$ , we get:

$$1 - p_\theta(\tilde{\mathbf{y}}_t | \mathbf{z}_t, \mathbf{x}) \leq 1 - p_\theta(\mathbf{y}' | \mathbf{z}_t, \mathbf{x}) \leq -\log p_\theta(\mathbf{y}' | \mathbf{z}_t, \mathbf{x}). \quad (19)$$

Since predictions factorize over tokens and unmasked positions are observed, by calibration assumption only masked positions contribute:

$$-\log p_\theta(\mathbf{y}' | \mathbf{z}_t, \mathbf{x}) = \sum_{i \in \mathcal{M}_t} -\log p_\theta(y'_i | \mathbf{z}_t, \mathbf{x}). \quad (20)$$

Taking expectations over  $(\mathbf{z}_t, \mathbf{x}, \mathbf{y}')$  and applying equation 19 and 20,

$$\mathbb{E}_{\mathbf{z}_t, \mathbf{x}} [1 - p_\theta(\tilde{\mathbf{y}}_t | \mathbf{z}_t, \mathbf{x})] \leq \mathbb{E}_{\mathbf{y}', \mathbf{z}_t, \mathbf{x}} [-\log p_\theta(\mathbf{y}' | \mathbf{z}_t, \mathbf{x})] = \mathbb{E}_{\mathbf{y}', \mathbf{z}_t, \mathbf{x}} \left[ \sum_{i \in \mathcal{M}_{t_k}} -\log p_\theta(y'_i | \tilde{\mathbf{y}}_{t_k}, \mathbf{x}) \right].$$

Having equations 18 and 16 and changing notation  $\mathbf{y}' = \mathbf{y}$ , we get:

$$\mathbb{P}(\tilde{\mathbf{y}}_t \neq \mathbf{y}) \leq \mathbb{E}_{\mathbf{y}, \mathbf{z}_t, \mathbf{x}} \left[ \sum_{i \in \mathcal{M}_{t_k}} -\log p_\theta(y_i | \tilde{\mathbf{y}}_{t_k}, \mathbf{x}) \right] = \frac{t}{T} \mathcal{L}_t^{\text{discr.}}(\theta) \quad (21)$$

Plugging this bound back into the expectation of the metric:

$$\mathbb{E}[\mathbf{u}_{\text{AD}}(\mathbf{x}, \mathbf{y})] \leq \frac{1}{T} \sum_{t=1}^T \frac{t}{T} \mathcal{L}_t^{\text{discr.}}(\theta) \quad (22)$$

Since  $\frac{t}{T} \leq 1, \forall t$ , we have:

$$\mathbb{E}[\mathbf{u}_{\text{AD}}(\mathbf{x}, \mathbf{y})] \leq \frac{1}{T} \sum_{t=1}^T \frac{t}{T} \mathcal{L}_t^{\text{discr.}}(\theta) \leq \frac{1}{T} \sum_{t=1}^T \mathcal{L}_t^{\text{discr.}}(\theta) = \mathcal{L}^{\text{discr.}}(\theta) \quad (23)$$

By taking  $T \rightarrow \infty$  gives us:

$$\mathbb{E}[\mathbf{u}_{\text{AD}}(\mathbf{x}, \mathbf{y})] \leq \mathcal{L}(\theta), \quad (24)$$

which completes the proof.

## A.2 Proof of Proposition 1

Since  $w_t = t/T$ , we have  $1/T \leq w_t \leq 1$  for all  $t$ . Because  $D(\tilde{\mathbf{y}}_t, \mathbf{y}) \geq 0$ , it follows that

$$\frac{1}{T}D(\tilde{\mathbf{y}}_t, \mathbf{y}) \leq w_t D(\tilde{\mathbf{y}}_t, \mathbf{y}) \leq D(\tilde{\mathbf{y}}_t, \mathbf{y}). \quad (25)$$

Averaging over  $t = 1, \dots, T$  gives

$$\frac{1}{T} \left( \frac{1}{T} \sum_{t=1}^T D(\tilde{\mathbf{y}}_t, \mathbf{y}) \right) \leq \frac{1}{T} \sum_{t=1}^T w_t D(\tilde{\mathbf{y}}_t, \mathbf{y}) \leq \frac{1}{T} \sum_{t=1}^T D(\tilde{\mathbf{y}}_t, \mathbf{y}). \quad (26)$$

Using the definitions of  $\mathbf{u}_{\text{AD}}$  and  $\mathbf{u}_{\text{AD}}^{\text{prog}}$  completes the proof.

## B Detailed Results

### B.1 Results for LLaDa-7B-v1.5

UQ Method	XSum	SamSum	WMT14	WMT19	CoQA	TriviaQA	MMLU	GSM8k	Mean
MCNSE	-0.07	0.07	0.29	0.25	-0.00	0.08	0.30	0.06	0.12
MCNSE-MCNLL	0.18	0.14	0.50	0.57	0.17	0.25	-0.03	0.19	0.25
SemanticEntropy	-0.04	0.15	0.35	0.36	0.04	0.11	0.42	0.13	0.19
SemanticEntropy-MCNLL	0.20	0.17	0.39	0.45	0.22	0.32	0.09	0.31	0.27
SemanticDensity	0.21	0.27	0.42	0.45	0.09	0.44	0.11	0.08	0.26
SemanticDensity-MCNLL	0.21	0.28	0.42	0.45	0.11	0.43	0.13	0.05	0.26
CoCoA-MSP	0.00	0.16	0.32	0.33	0.08	0.17	0.42	0.17	0.21
CoCoA-MCNLL	0.23	0.21	0.51	0.57	0.31	0.50	0.41	0.28	0.38

Table 4: PRR $\uparrow$  for LLaDA-7B-v1.5 across various tasks for sampling-based baselines from standard autoregressive LLMs, where MCNLL is used instead of sequence probability (see Tab. 10 for the Dream model). Darker color indicates better results.

UQ Method	XSum	SamSum	WMT14	WMT19	CoQA	TriviaQA	MMLU	GSM8k	Mean
D-LexSim	0.09	-0.03	0.10	0.18	0.21	0.16	0.02	-0.02	0.09
D-DegMat	0.09	0.01	0.11	0.21	0.20	0.41	0.00	-0.00	0.13
D-EigVal	0.09	0.02	0.12	0.20	0.21	0.44	0.04	0.00	0.14
D-Ecc	0.10	0.01	0.14	0.22	0.23	0.32	0.02	0.01	0.13
D-KLE	-0.07	-0.07	-0.17	-0.20	-0.09	0.21	0.02	-0.11	-0.06
D-LUQ	0.08	0.02	0.08	0.18	0.17	0.40	0.02	0.02	0.12

Table 5: PRR $\uparrow$  for LLaDA-7B-v1.5 across various tasks for sampling-based baselines from standard autoregressive LLMs, where generated trajectory is used instead of sampling answers (see Tab. 11 for the Dream model). Darker color indicates better results.

UQ Method	XSum	SamSum	WMT14	WMT19	CoQA	TriviaQA	MMLU	GSM8k	Mean
MSP	-0.08	0.11	0.20	0.16	-0.02	0.05	0.34	0.09	0.10
SAR	0.07	0.21	0.43	0.46	0.20	0.46	0.42	0.16	0.30
CoCoA-MTE	0.09	0.18	0.51	0.53	0.17	0.26	0.43	0.20	0.30
KLE	0.22	0.24	0.44	0.48	0.27	0.60	0.43	0.17	0.36
TAD	0.20	0.38	0.54	0.51	0.14	0.51	0.34	0.35	0.37
MCNLL	0.17	0.18	0.29	0.32	0.24	0.31	0.35	0.23	0.26
NFE	0.15	0.17	0.31	0.31	0.22	0.18	0.02	0.29	0.21
AD-Full	0.09	0.22	0.25	0.36	0.29	0.39	-0.05	0.03	0.20
CommitNLL	0.18	0.19	0.39	0.43	0.22	0.43	0.47	0.30	0.33
CoCoA-MCNLL	0.23	0.21	0.51	0.57	0.31	0.50	0.41	0.28	0.38
CoCoA-MCNLL-Norm	0.23	0.30	0.42	0.51	0.28	0.37	0.41	0.17	0.34
D-CoCoA-G	0.21	0.26	0.42	0.53	0.32	0.36	0.35	0.19	0.33
D-CoCoA-L	0.22	0.23	0.41	0.48	0.28	0.53	0.46	0.23	0.35

Table 6: PRR $\uparrow$  for LLaDA-7B-v1.5 across various tasks for D-CoCoA methods, comparing the best method from each category (see Tab. 12 for the Dream model). Darker color indicates better results.

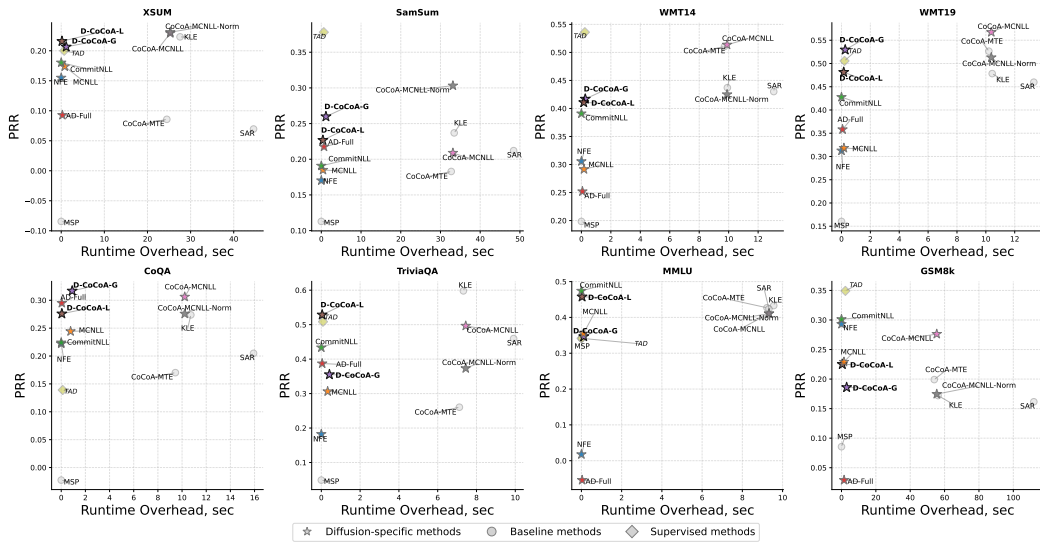


Figure 3: Comparison of uncertainty quantification performance (PRR $\uparrow$ ) versus computational complexity (Time in seconds $\downarrow$ ) across eight benchmark datasets for the LLaDa-1.5 model (see Fig. 4 for the Dream model).

## B.2 Results for Dream

UQ Method	XSum	SamSum	WMT14	WMT19	CoQA	TriviaQA	MMLU	GSM8k	Mean
MSP	-0.05	0.05	-0.07	-0.04	0.17	0.15	0.71	0.16	0.13
MTE	0.15	0.25	0.41	0.44	0.05	0.19	0.62	0.14	0.28
Perplexity	0.03	0.25	0.15	0.18	0.13	0.12	0.56	0.10	0.19
AttScore	-0.01	0.05	-0.14	-0.12	0.05	0.13	0.03	0.19	0.02
CCP	-0.03	0.09	-0.07	-0.03	0.18	0.15	0.47	0.14	0.11
RAUQ	0.02	0.12	0.08	0.11	0.17	0.03	0.55	0.09	0.15
MCNSE	0.06	0.13	0.29	0.36	0.21	0.52	0.70	0.02	0.29
SemanticEntropy	-0.03	0.02	0.09	0.21	0.27	0.58	0.76	0.20	0.26
SAR	0.14	0.20	0.39	0.47	0.28	0.60	0.73	0.33	0.39
EigenScore	0.08	0.14	0.47	0.56	0.34	0.65	0.30	0.58	0.39
CoCoA-MTE	0.25	0.28	0.72	0.76	0.24	0.58	0.74	0.41	0.50
SemanticDensity	0.17	0.21	0.60	0.67	0.12	0.61	0.05	0.09	0.31
LUQ	0.32	0.30	0.46	0.50	0.31	0.66	0.64	0.59	0.47
KLE	0.34	0.29	0.47	0.55	0.32	0.67	0.52	0.60	0.47
DegMat	0.23	0.24	0.49	0.57	0.32	0.67	0.44	0.58	0.44
SAPLMA	0.24	0.26	0.77	0.77	0.01	0.63	0.40	0.22	0.41
SATRMD	0.23	0.22	0.54	0.60	0.19	0.33	0.75	0.18	0.38
LookBackLens	0.34	0.29	0.72	0.74	0.32	0.64	0.60	0.31	0.49
TAD	0.44	0.42	0.57	0.48	0.23	0.51	0.02	0.39	0.38

Table 7: PRR $\uparrow$  for the Dream model for various tasks for the considered classical autoregressive methods (see Tab. 1 for the LLaDA-7B-v1.5 model). Warmer color indicates better results.

UQ Method	XSum	SamSum	WMT14	WMT19	CoQA	TriviaQA	MMLU	GSM8k	Mean
MCNLL	0.09	0.03	0.00	0.06	0.25	0.48	0.75	0.28	0.24
MCNLL-Norm	0.22	0.31	0.45	0.46	0.09	0.37	0.75	0.23	0.36
NFE	0.00	-0.02	0.38	0.49	0.35	0.50	0.03	0.35	0.26
Remask	0.00	-0.03	0.33	0.43	0.33	0.45	0.03	0.36	0.24
FlipCount	-0.02	-0.04	0.05	0.11	0.25	0.34	0.19	0.28	0.15
TrajNLL	0.08	0.01	0.24	0.37	0.30	0.59	0.52	0.35	0.31
TrajEntropy	0.11	0.03	0.29	0.40	0.30	0.55	0.72	0.38	0.35
CommitNLL	0.11	0.03	0.40	0.53	0.40	0.68	0.52	0.39	0.38

Table 8: PRR $\uparrow$  for the Dream model for various diffusion-specific UQ baselines (see Tab. 2 for the LLaDA-7B-v1.5 model). Darker color indicates better results.

UQ Method	XSum	SamSum	WMT14	WMT19	CoQA	TriviaQA	MMLU	GSM8k	Mean
AD-Block	0.18	0.16	0.51	0.57	0.26	0.44	0.71	-0.00	0.35
WeightedAD-Block	0.14	0.11	0.53	0.58	0.31	0.49	0.70	0.25	0.39
AD-LastBlock	0.07	0.06	0.00	-0.00	0.26	0.44	0.71	-0.02	0.19
WeightedAD-LastBlock	0.10	0.05	0.00	-0.00	0.31	0.49	0.70	0.02	0.21
AD-LastBlockPrefix	0.00	0.09	0.39	0.38	0.26	0.44	0.71	0.09	0.29
WeightedAD-LastBlockPrefix	-0.04	0.09	0.39	0.38	0.31	0.49	0.70	0.13	0.30
AD-Full	0.05	0.16	0.56	0.62	0.26	0.44	0.71	0.09	0.36
WeightedAD-Full	0.07	0.16	0.55	0.61	0.31	0.49	0.70	0.08	0.37

Table 9: PRR $\uparrow$  for the Dream model for various trajectory dissimilarity baselines (see Tab. 3 for the LLaDA-7B-v1.5 model). Darker color indicates better results.

UQ Method	XSum	SamSum	WMT14	WMT19	CoQA	TriviaQA	MMLU	GSM8k	Mean
MCNSE	0.06	0.13	0.29	0.36	0.21	0.52	0.70	0.02	0.29
MCNSE-MCNLL	0.14	0.06	0.35	0.32	-0.10	0.15	-0.24	-0.03	0.08
SemanticEntropy	-0.03	0.02	0.09	0.21	0.27	0.58	0.76	0.20	0.26
SemanticEntropy-MCNLL	-0.05	-0.03	-0.09	-0.06	0.17	0.29	0.69	0.25	0.15
SemanticDensity	0.17	0.21	0.60	0.67	0.12	0.61	0.05	0.09	0.31
SemanticDensity-MCNLL	0.15	0.25	0.60	0.66	0.22	0.46	0.69	0.18	0.40
CoCoA-MSP	0.05	0.10	0.30	0.35	0.28	0.46	0.76	0.30	0.32
CoCoA-MCNLL	0.19	0.09	0.49	0.52	0.35	0.67	0.74	0.42	0.43

Table 10: PRR $\uparrow$  for Dream across various tasks for sampling-based baselines from standard autoregressive LLMs, where MCNLL is used instead of sequence probability (see Tab. 4 for the LLaDA-7B-v1.5 model). Darker color indicates better results.

UQ Method	XSum	SamSum	WMT14	WMT19	CoQA	TriviaQA	MMLU	GSM8k	Mean
D-LexSim	-0.03	0.04	0.02	0.02	0.21	0.12	0.66	0.03	0.13
D-DegMat	-0.04	0.04	0.40	0.38	0.28	0.45	0.39	0.05	0.24
D-EigVal	-0.03	-0.04	-0.00	0.04	0.30	0.46	0.68	0.03	0.18
D-Ecc	-0.05	0.04	0.00	0.02	0.29	0.44	0.68	0.04	0.18
D-KLE	0.01	0.05	0.40	0.38	-0.18	0.13	0.67	-0.02	0.18
D-LUQ	-0.02	0.11	0.45	0.45	0.24	0.39	0.63	0.06	0.29

Table 11: PRR $\uparrow$  for Dream across various tasks for sampling-based baselines from standard autoregressive LLMs, where generated trajectory is used instead of sampling answers (see Tab. 5 for the LLaDA-7B-v1.5 model). Darker color indicates better results.

UQ Method	XSum	SamSum	WMT14	WMT19	CoQA	TriviaQA	MMLU	GSM8k	Mean
MSP	-0.05	0.05	-0.07	-0.04	0.17	0.15	0.71	0.16	0.13
SAR	0.14	0.20	0.39	0.47	0.28	0.60	0.73	0.33	0.39
CoCoA-MTE	0.25	0.28	0.72	0.76	0.24	0.58	0.74	0.41	0.50
KLE	0.34	0.29	0.47	0.55	0.32	0.67	0.52	0.60	0.47
TAD	0.44	0.42	0.57	0.48	0.23	0.51	0.02	0.39	0.38
MCNLL	0.09	0.03	0.00	0.06	0.25	0.48	0.75	0.28	0.24
NFE	0.00	-0.02	0.38	0.49	0.35	0.50	0.03	0.35	0.26
AD-Full	0.05	0.16	0.56	0.62	0.26	0.44	0.71	0.09	0.36
CommitNLL	0.11	0.03	0.40	0.53	0.40	0.68	0.52	0.39	0.38
CoCoA-MCNLL	0.19	0.09	0.49	0.52	0.35	0.67	0.74	0.42	0.43
CoCoA-MCNLL-Norm	0.29	0.30	0.71	0.72	0.29	0.67	0.74	0.48	0.53
D-CoCoA-G	0.14	0.22	0.64	0.68	0.34	0.62	0.75	0.33	0.47
D-CoCoA-L	0.20	0.08	0.55	0.64	0.37	0.65	0.78	0.43	0.46

Table 12: PRR $\uparrow$  for the Dream across various tasks for D-CoCoA methods, comparing the best method from each category (see Tab. 6 for the LLaDA-7B-v1.5 model). Darker color indicates better results.

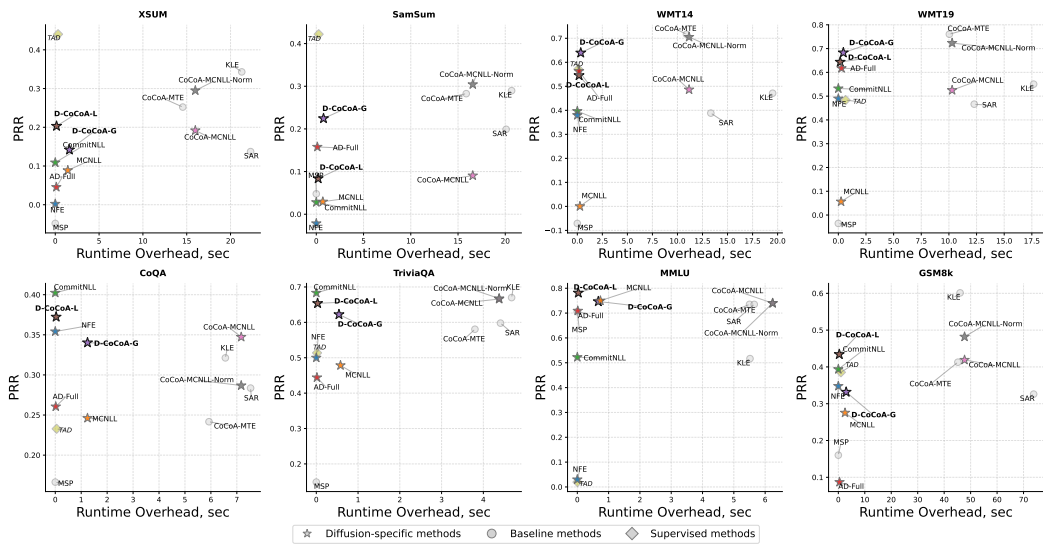


Figure 4: Comparison of uncertainty quantification performance (PRR $\uparrow$ ) versus computational complexity (Time in seconds $\downarrow$ ) across eight benchmark datasets for the Dream model (see Fig. 3 for the LLaDa-1.5 model).

### B.3 Results Using the ROC-AUC Metric

The averaged results evaluated using the ROC-AUC metric are presented in Figure 5. Detailed results for each dataset are presented in Figures 6 and 7 for LLaDA and Dream, respectively.

For all generation quality metrics other than accuracy, we compute scores by thresholding the original continuous values to obtain discrete labels. The thresholds were empirically determined as follows: 0.3 for QA and Summ, and 0.8 for MT. We observe trends similar to those seen with the PRR metric. D-CoCoA methods show the best performanceefficiency trade-off. Among diffusion-based methods, D-CoCoA-G achieves the best average performance for LLaDA, and D-CoCoA-L for Dream. While absolute values differ slightly from PRR, these results again highlight the strong suitability of the proposed method for efficient LLDMs.

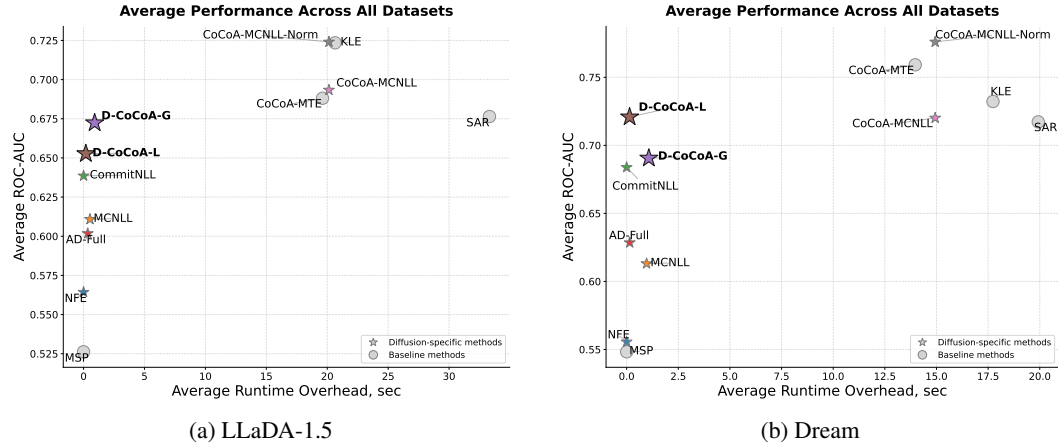


Figure 5: Comparison of uncertainty quantification performance (ROC-AUC $\uparrow$ ) versus computational complexity (Time in seconds $\downarrow$ ) averaged across all datasets.

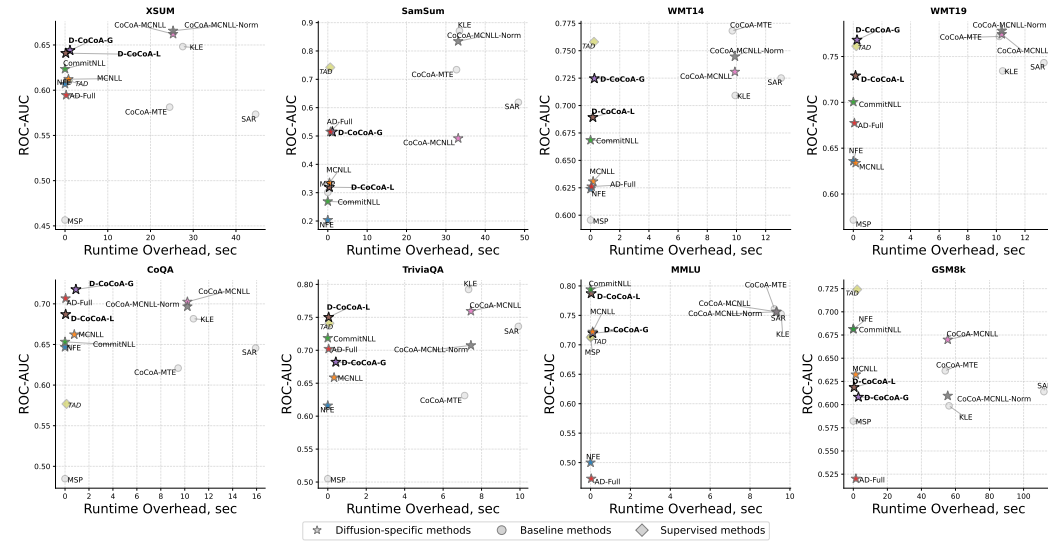


Figure 6: Comparison of uncertainty quantification performance (ROC-AUC $\uparrow$ ) versus computational complexity (Time in seconds $\downarrow$ ) across eight benchmark datasets for the LLaDA-1.5 model (see Fig. 7 for the Dream model).

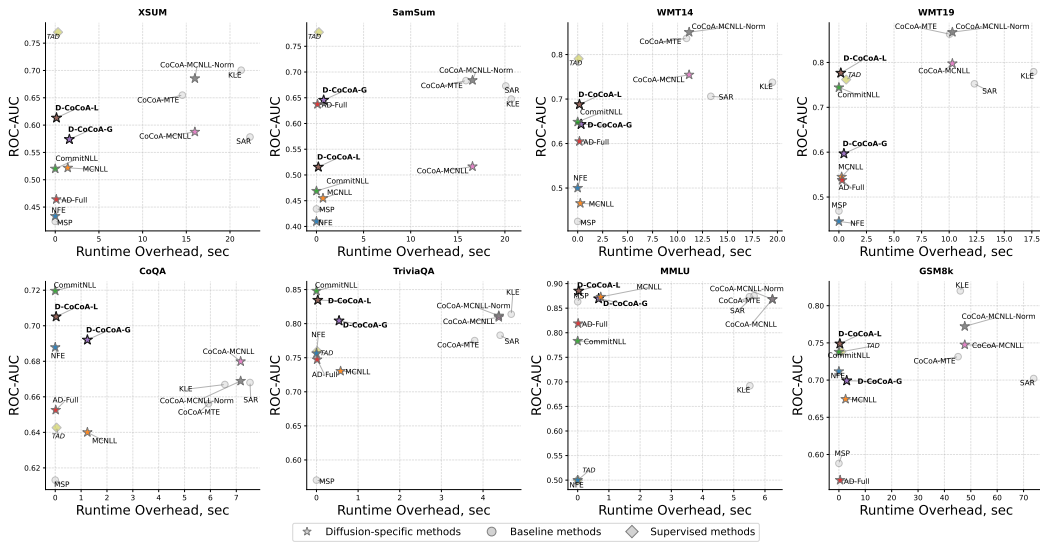


Figure 7: Comparison of uncertainty quantification performance (ROC-AUC $\uparrow$ ) versus computational complexity (Time in seconds $\downarrow$ ) across eight benchmark datasets for the Dream model (see Fig. 6 for the LLaDa-1.5 model).

## C Ablation Studies

To understand the contributions of individual components of D-CoCoA methods, we conduct four ablation studies.

**Sources of likelihood.** Table 13 in Appendix C reports ablation results in which the information-based component of D-CoCoA-G and D-CoCoA-L is replaced with alternative scoring methods: MCNLL, trajectory likelihood (both variants), and normalized/unnormalized MCNLL.

The original D-CoCoA-G outperforms its variants on average, with particular strength in long-form tasks such as summarization and translation. Its TrajNLL variant provides the best results, surpassing the best sampling-based baseline on CoQA and MMLU, though MCNLL offers the most consistent performance overall. The original D-CoCoA-L likewise achieves the best performance among its variants on average, achieving top results on all datasets except CoQA.

**Trajectory aggregation.** Table 14 in Appendix C evaluates D-CoCoA under different definitions of  $z_t$  as stated in Section 3. These results confirm that the full generation trajectory is optimal for D-CoCoA-G, and individual block-wise averaging for D-CoCoA-L. Overall, performance remains stable across all alternatives, with no significant degradation.

**Trajectory similarity functions.** Table 15 in Appendix C presents D-CoCoA-NFE results under different similarity functions (DeBERTa NLI and Cross-Encoder with RoBERTa) and weighted or unweighted aggregation. These results demonstrate the overall consistency of the proposed methods. Replacing the Cross-Encoder with the NLI model reduces average performance by at most 1% for both variants. Progressive weighted scoring yields marginal WMT gains for D-CoCoA-G but degrades QA performance, leaving the overall unchanged, and slightly reduces performance across all datasets for D-CoCoA-L.

**Additional diffusion statistic.** Table 16 in Appendix C evaluates the contribution of the NFE component in D-CoCoA. For D-CoCoA-G, incorporating NFE yields consistent and substantial improvements, confirming that it captures information distinct from other global trajectory-based signals. For D-CoCoA-L, however, it slightly reduces performance on all datasets except GSM8k.

UQ Method	XSum	SamSum	WMT14	WMT19	CoQA	TriviaQA	MMLU	GSM8k	Mean
D-CoCoA-G (TrajNLL)	0.20	0.19	0.28	0.31	0.35	0.44	0.46	0.25	0.31
D-CoCoA-G (TrajEntropy)	0.20	0.19	0.30	0.34	0.34	0.46	0.43	0.25	0.31
D-CoCoA-G (MCNLL)	0.21	0.18	0.34	0.38	0.35	0.46	0.35	0.24	0.31
D-CoCoA-G (CommitNLL)	0.20	0.18	0.35	0.40	0.31	0.49	0.46	0.28	0.33
D-CoCoA-G	0.21	0.26	0.42	0.53	0.32	0.36	0.35	0.19	0.33
D-CoCoA-L (TrajNLL)	0.20	0.08	0.21	0.26	0.30	0.49	0.46	-0.04	0.25
D-CoCoA-L (TrajEntropy)	0.20	0.08	0.26	0.32	0.29	0.50	0.43	-0.03	0.26
D-CoCoA-L (MCNLL)	0.22	0.21	0.28	0.37	0.30	0.46	0.35	0.11	0.29
D-CoCoA-L (MCNLL-Norm)	0.20	0.07	0.19	0.26	0.27	0.29	0.35	-0.09	0.19
D-CoCoA-L	0.22	0.23	0.41	0.48	0.28	0.53	0.46	0.23	0.35

Table 13: PRR $\uparrow$  for LLaDA-7B-v1.5 across various tasks for D-CoCoA methods with various information-based components. Warmer color indicates better results.

UQ Method	XSum	SamSum	WMT14	WMT19	CoQA	TriviaQA	MMLU	GSM8k	Mean
D-CoCoA-G (Block-wise)	0.21	0.25	0.39	0.51	0.30	0.36	0.35	0.10	0.31
D-CoCoA-G (Last Block)	0.19	0.22	0.38	0.50	0.30	0.36	0.35	0.16	0.31
D-CoCoA-G (Last Block with prefix)	0.20	0.23	0.36	0.48	0.32	0.36	0.35	0.14	0.30
D-CoCoA-G	0.21	0.26	0.42	0.53	0.32	0.36	0.35	0.19	0.33
D-CoCoA-L (Full Trace)	0.21	0.19	0.36	0.43	0.33	0.53	0.46	0.25	0.34
D-CoCoA-L (Last Block)	0.20	0.19	0.38	0.46	0.28	0.53	0.46	0.21	0.34
D-CoCoA-L (Last Block with prefix)	0.20	0.21	0.37	0.47	0.33	0.53	0.46	0.17	0.34
D-CoCoA-L	0.22	0.23	0.41	0.48	0.28	0.53	0.46	0.23	0.35

Table 14: PRR $\uparrow$  for LLaDA-7B-v1.5 across various tasks for D-CoCoA methods with different trajectory block-wise aggregations. Darker color indicates better results.

UQ Method	XSum	SamSum	WMT14	WMT19	CoQA	TriviaQA	MMLU	GSM8k	Mean
D-CoCoA-G (Deberta Progress)	0.20	0.28	0.45	0.53	0.28	0.33	0.34	0.18	0.32
D-CoCoA-G (Deberta)	0.21	0.28	0.39	0.47	0.30	0.39	0.34	0.02	0.30
D-CoCoA-G (Progress)	0.19	0.26	0.45	0.54	0.28	0.30	0.35	0.21	0.32
D-CoCoA-G	0.21	0.26	0.42	0.53	0.32	0.36	0.35	0.19	0.33
D-CoCoA-L (Deberta Progress)	0.20	0.19	0.40	0.44	0.24	0.47	0.46	0.30	0.34
D-CoCoA-L (Deberta)	0.21	0.21	0.42	0.46	0.23	0.50	0.46	0.29	0.35
D-CoCoA-L (Progress)	0.19	0.19	0.40	0.44	0.25	0.49	0.46	0.30	0.34
D-CoCoA-L	0.22	0.23	0.41	0.48	0.28	0.53	0.46	0.23	0.35

Table 15: PRR $\uparrow$  for LLaDA-7B-v1.5 across various tasks for D-CoCoA-NFE with different similarity functions (DeBERTa NLI and Cross-Encoder with RoBERTa) and weighted or unweighted aggregation. Darker color indicates better results.

UQ Method	XSum	SamSum	WMT14	WMT19	CoQA	TriviaQA	MMLU	GSM8k	Mean
D-CoCoA-G (w/o NFE)	0.19	0.25	0.37	0.49	0.28	0.28	0.35	-0.01	0.28
D-CoCoA-G	0.21	0.26	0.42	0.53	0.32	0.36	0.35	0.19	0.33
D-CoCoA-L (with NFE)	0.21	0.20	0.37	0.42	0.27	0.49	0.46	0.28	0.34
D-CoCoA-L	0.22	0.23	0.41	0.48	0.28	0.53	0.46	0.23	0.35

Table 16: PRR $\uparrow$  for LLaDA-7B-v1.5 across various tasks for D-CoCoA-NFE with and without the NFE component. Darker color indicates better results.

## D Additional Details of Experimental Setup

### D.1 Implementation Details

We evaluate two models: LLaDA-1.5<sup>1</sup> (Nie et al., 2025) and Dream-v0-Instruct-7B<sup>2</sup> (Ye et al., 2025), both 7B-parameter masked diffusion LLMs fine-tuned for instruction following. To reflect practical inference conditions, generation is performed using KV cache and Parallel Decoding (Wu et al., 2026), following the default configuration of FastLLM. We use a factor-based parallel decoding strategy with a factor of 1. Detailed generation hyperparameters are presented in Table 17 in Appendix D.3.

For semantic evaluation, we use two pretrained discriminative models: RoBERTa-large<sup>3</sup>, which produces a continuous similarity score in  $[0, 1]$ , and DeBERTa-large<sup>4</sup>, from which we extract the softmax probability assigned to the entailment class. RoBERTa-large serves as the default similarity function in the proposed D-CoCoA methods. Both models are used in inference-only mode without fine-tuning.

All supervised methods are evaluated in an in-domain setup, where uncertainty predictors are trained on 1000 instances from the training split of the same dataset. This establishes an upper bound on supervised performance. In practice, such methods tend to degrade substantially in out-of-domain scenarios (Vazhentsev et al., 2025a).

For all uses of MCNLL and MCNLL-Norm, both as standalone methods and as components of other methods, we use  $N_{mc} = 16$ . While previous work (Nie et al., 2025) suggests using  $N_{mc} = 128$ , we observe that it usually does not introduce additional performance gains, while requiring substantially more runtime. For MMLU, we do not perform masking since only one token is generated.

All experiments are conducted on an NVIDIA A100 40GB and an NVIDIA RTX 6000 48GB GPUs using single-batch inference. Figures 3 and 4 in Appendix B reports the average runtime overhead per instance for each UQ method relative to standard LLM inference without UQ. Figure 2 reports the same metric averaged across datasets.

<sup>1</sup><https://huggingface.co/GSAI-ML/LLaDA-1.5>

<sup>2</sup><https://huggingface.co/Dream-org/Dream-v0-Instruct-7B>

<sup>3</sup><https://huggingface.co/cross-encoder/stsb-roberta-large>

<sup>4</sup><https://huggingface.co/microsoft/deberta-large-mnli>

## D.2 Detailed Description of UQ Baselines

We evaluate seventeen unsupervised and four supervised UQ baselines, originally developed for standard autoregressive LLMs, on diffusion LLMs.

This evaluation includes simple unsupervised baselines such as Maximum Sequence Probability (MSP), Perplexity, and Mean Token Entropy (MTE; Fomicheva et al., 2020). While diffusion probabilities are not trained to yield meaningful sequence-level products, they can still be computed.

Among single forward-pass state-of-the-art baselines for white-box LLMs, we evaluate Claim-Conditioned Probability (CCP; Fadeeva et al., 2024), Attention Score (Sriramanan et al., 2024), and Recurrent Attention-based Uncertainty Quantification (RAUQ; Vazhentsev et al., 2025b).

Among sampling-based state-of-the-art baselines for white-box LLMs, we evaluate Monte Carlo Normalized Sequence Entropy (MCNSE; Malinin and Gales, 2021), Semantic Entropy (Kuhn et al., 2023), Shifting Attention to Relevance (SAR; Duan et al., 2024), Semantic Density (Qiu and Mikkulainen, 2024), EigenScore (Chen et al., 2024), and CoCoA with MTE (Vashurin et al., 2025b).

Moreover, we consider UQ methods for black-box LLMs, including lexical similarity based on ROUGE-L (Fomicheva et al., 2020), Long-text Uncertainty Quantification (LUQ; Zhang et al., 2024), and methods from (Lin et al., 2024): Degree Matrix (DegMat), Eccentricity (Ecc), and the sum of eigenvalues of the graph Laplacian (EigVal).

Additionally, we consider four supervised state-of-the-art baselines for white-box LLMs. These include two methods based on hidden states, Statement Accuracy Prediction based on Language Model Activations (SAPLMA; Azaria and Mitchell, 2023) and Supervised Average Token-level Relative Mahalanobis Distance (SATRMD; Vazhentsev et al., 2025c), and two methods based on attention weights, Lookback Lens (Chuang et al., 2024) and Trainable Attention-based Dependency (TAD; Vazhentsev et al., 2025a).

## D.3 Dataset and Generation Statistics

We perform experiments across three representative generation tasks: question answering (QA), text summarization (Summ), and machine translation (MT). For QA, we consider four datasets covering diverse domains and reasoning types: MMLU (Hendrycks et al., 2021), TriviaQA (Joshi et al., 2017), CoQA (Reddy et al., 2019), and GSM8k (Cobbe et al., 2021). For summarization, we use SamSum (Gliwa et al., 2019) and XSum (Narayan et al., 2018), representing dialog, news, and extreme summarization settings. For machine translation, we evaluate on WMT benchmarks: German-English (WMT19; Barrault et al., 2019) and French-English (WMT14; Bojar et al., 2014).

We follow the default inference configuration of FastDLLM (Wu et al., 2026) for both models. The datasets and prompts are taken from the LM-Polygraph framework<sup>5</sup> (Fadeeva et al., 2023). Dataset statistics and inference hyperparameters are presented in Table 17.

Task	Dataset	Number of test samples	N-shot	Generation length	Block length	Num. of diff. steps
QA	MMLU	2000	5	3	3	256
	TriviaQA	2000	5	20	5	
	CoQA	2000	all preceding questions	20	5	
	GSM8k	1319		5	256	
ATS	SamSum	819	0	128	32	
	XSum	2000	0	128	32	
NMT	WMT19 (De-En)	2000	0	128	32	
	WMT14 (Fr-En)	2000	0	128	32	

Table 17: Statistics of the datasets and generation parameters of the used LLMs. For all datasets, we do not limit the maximum input length. For all texts, we use greedy generation (temperature = 0); for sampling, we use temperature 1 to obtain diverse outputs.

<sup>5</sup><https://huggingface.co/LM-Polygraph/datasets>

## **E Limitations**

While our evaluation covers the most prominent publicly available open-weighted discrete masked LLDMs at the time of submission, broader evaluation across other diffusion paradigms and model scales remains future work due to the currently limited availability of such models. Our theoretical results rely on standard assumptions that may not always hold exactly in practice, potentially loosening the stated bounds in some settings. Finally, the reported computational overhead is specific to the hardware configuration and inference algorithm used in our experiments and may vary across different setups.

## **F Broader Impact**

This work presents a systematic study of uncertainty quantification in discrete masked LLDMs, enabling reliable hallucination detection without requiring task-specific labels or repeated sampling. We consider this a meaningful step toward more trustworthy deployment of diffusion-based language models, particularly in safety-critical applications. In our experiments, we use open-weight models and publicly available datasets that are not focused on harmful content. The explored approaches pose no negative societal impact, as they do not rely on sensitive data, user annotations, or other elements that could raise ethical concerns.

## NeurIPS Paper Checklist

### 1. Claims

Question: Do the main claims made in the abstract and introduction accurately reflect the paper’s contributions and scope?

Answer: [Yes]

Justification: Yes, the claims made in the abstract and introduction are precisely supported by the description of the method in Section 3 and by the experimental evaluations in Section 4.

Guidelines:

- The answer [N/A] means that the abstract and introduction do not include the claims made in the paper.
- The abstract and/or introduction should clearly state the claims made, including the contributions made in the paper and important assumptions and limitations. A [No] or [N/A] answer to this question will not be perceived well by the reviewers.
- The claims made should match theoretical and experimental results, and reflect how much the results can be expected to generalize to other settings.
- It is fine to include aspirational goals as motivation as long as it is clear that these goals are not attained by the paper.

### 2. Limitations

Question: Does the paper discuss the limitations of the work performed by the authors?

Answer: [Yes]

Justification: Yes, the limitations of the work are discussed in Appendix E.

Guidelines:

- The answer [N/A] means that the paper has no limitation while the answer [No] means that the paper has limitations, but those are not discussed in the paper.
- The authors are encouraged to create a separate “Limitations” section in their paper.
- The paper should point out any strong assumptions and how robust the results are to violations of these assumptions (e.g., independence assumptions, noiseless settings, model well-specification, asymptotic approximations only holding locally). The authors should reflect on how these assumptions might be violated in practice and what the implications would be.
- The authors should reflect on the scope of the claims made, e.g., if the approach was only tested on a few datasets or with a few runs. In general, empirical results often depend on implicit assumptions, which should be articulated.
- The authors should reflect on the factors that influence the performance of the approach. For example, a facial recognition algorithm may perform poorly when image resolution is low or images are taken in low lighting. Or a speech-to-text system might not be used reliably to provide closed captions for online lectures because it fails to handle technical jargon.
- The authors should discuss the computational efficiency of the proposed algorithms and how they scale with dataset size.
- If applicable, the authors should discuss possible limitations of their approach to address problems of privacy and fairness.
- While the authors might fear that complete honesty about limitations might be used by reviewers as grounds for rejection, a worse outcome might be that reviewers discover limitations that aren’t acknowledged in the paper. The authors should use their best judgment and recognize that individual actions in favor of transparency play an important role in developing norms that preserve the integrity of the community. Reviewers will be specifically instructed to not penalize honesty concerning limitations.

### 3. Theory assumptions and proofs

Question: For each theoretical result, does the paper provide the full set of assumptions and a complete (and correct) proof?

Answer: [Yes]

Justification: Yes, the paper provides theoretical results in Theorem 1, with the full set of assumptions in Section 3.3 and complete proof in Appendix A.

Guidelines:

- The answer [N/A] means that the paper does not include theoretical results.
- All the theorems, formulas, and proofs in the paper should be numbered and cross-referenced.
- All assumptions should be clearly stated or referenced in the statement of any theorems.
- The proofs can either appear in the main paper or the supplemental material, but if they appear in the supplemental material, the authors are encouraged to provide a short proof sketch to provide intuition.
- Inversely, any informal proof provided in the core of the paper should be complemented by formal proofs provided in appendix or supplemental material.
- Theorems and Lemmas that the proof relies upon should be properly referenced.

#### 4. Experimental result reproducibility

Question: Does the paper fully disclose all the information needed to reproduce the main experimental results of the paper to the extent that it affects the main claims and/or conclusions of the paper (regardless of whether the code and data are provided or not)?

Answer: [Yes]

Justification: All necessary details for reproducing the experimental results, including hyperparameters, dataset statistics, model checkpoints, hardware configuration, and implementation details, are provided in Section 4 and in Appendix D to ensure full reproducibility.

Guidelines:

- The answer [N/A] means that the paper does not include experiments.
- If the paper includes experiments, a [No] answer to this question will not be perceived well by the reviewers: Making the paper reproducible is important, regardless of whether the code and data are provided or not.
- If the contribution is a dataset and/or model, the authors should describe the steps taken to make their results reproducible or verifiable.
- Depending on the contribution, reproducibility can be accomplished in various ways. For example, if the contribution is a novel architecture, describing the architecture fully might suffice, or if the contribution is a specific model and empirical evaluation, it may be necessary to either make it possible for others to replicate the model with the same dataset, or provide access to the model. In general, releasing code and data is often one good way to accomplish this, but reproducibility can also be provided via detailed instructions for how to replicate the results, access to a hosted model (e.g., in the case of a large language model), releasing of a model checkpoint, or other means that are appropriate to the research performed.
- While NeurIPS does not require releasing code, the conference does require all submissions to provide some reasonable avenue for reproducibility, which may depend on the nature of the contribution. For example
  - (a) If the contribution is primarily a new algorithm, the paper should make it clear how to reproduce that algorithm.
  - (b) If the contribution is primarily a new model architecture, the paper should describe the architecture clearly and fully.
  - (c) If the contribution is a new model (e.g., a large language model), then there should either be a way to access this model for reproducing the results or a way to reproduce the model (e.g., with an open-source dataset or instructions for how to construct the dataset).
  - (d) We recognize that reproducibility may be tricky in some cases, in which case authors are welcome to describe the particular way they provide for reproducibility. In the case of closed-source models, it may be that access to the model is limited in

some way (e.g., to registered users), but it should be possible for other researchers to have some path to reproducing or verifying the results.

#### 5. Open access to data and code

Question: Does the paper provide open access to the data and code, with sufficient instructions to faithfully reproduce the main experimental results, as described in supplemental material?

Answer: [Yes]

Justification: The implementation code will be anonymously included in the supplementary materials to ensure transparency and reproducibility.

Guidelines:

- The answer [N/A] means that paper does not include experiments requiring code.
- Please see the NeurIPS code and data submission guidelines (<https://neurips.cc/public/guides/CodeSubmissionPolicy>) for more details.
- While we encourage the release of code and data, we understand that this might not be possible, so [No] is an acceptable answer. Papers cannot be rejected simply for not including code, unless this is central to the contribution (e.g., for a new open-source benchmark).
- The instructions should contain the exact command and environment needed to run to reproduce the results. See the NeurIPS code and data submission guidelines (<https://neurips.cc/public/guides/CodeSubmissionPolicy>) for more details.
- The authors should provide instructions on data access and preparation, including how to access the raw data, preprocessed data, intermediate data, and generated data, etc.
- The authors should provide scripts to reproduce all experimental results for the new proposed method and baselines. If only a subset of experiments are reproducible, they should state which ones are omitted from the script and why.
- At submission time, to preserve anonymity, the authors should release anonymized versions (if applicable).
- Providing as much information as possible in supplemental material (appended to the paper) is recommended, but including URLs to data and code is permitted.

#### 6. Experimental setting/details

Question: Does the paper specify all the training and test details (e.g., data splits, hyperparameters, how they were chosen, type of optimizer) necessary to understand the results?

Answer: [Yes]

Justification: All relevant details of the testing experiments are provided in Section 4 and Appendix D. No model training is performed in this work.

Guidelines:

- The answer [N/A] means that the paper does not include experiments.
- The experimental setting should be presented in the core of the paper to a level of detail that is necessary to appreciate the results and make sense of them.
- The full details can be provided either with the code, in appendix, or as supplemental material.

#### 7. Experiment statistical significance

Question: Does the paper report error bars suitably and correctly defined or other appropriate information about the statistical significance of the experiments?

Answer: [Yes]

Justification: Reliability of the results is ensured by fixing random seeds and using greedy decoding, which leads to deterministic generation. To further demonstrate the robustness of our findings, we conducted experiments across two LLMs and eight datasets from diverse domains and tasks.

Guidelines:

- The answer [N/A] means that the paper does not include experiments.

- The authors should answer [Yes] if the results are accompanied by error bars, confidence intervals, or statistical significance tests, at least for the experiments that support the main claims of the paper.
- The factors of variability that the error bars are capturing should be clearly stated (for example, train/test split, initialization, random drawing of some parameter, or overall run with given experimental conditions).
- The method for calculating the error bars should be explained (closed form formula, call to a library function, bootstrap, etc.)
- The assumptions made should be given (e.g., Normally distributed errors).
- It should be clear whether the error bar is the standard deviation or the standard error of the mean.
- It is OK to report 1-sigma error bars, but one should state it. The authors should preferably report a 2-sigma error bar than state that they have a 96% CI, if the hypothesis of Normality of errors is not verified.
- For asymmetric distributions, the authors should be careful not to show in tables or figures symmetric error bars that would yield results that are out of range (e.g., negative error rates).
- If error bars are reported in tables or plots, the authors should explain in the text how they were calculated and reference the corresponding figures or tables in the text.

#### 8. Experiments compute resources

Question: For each experiment, does the paper provide sufficient information on the computer resources (type of compute workers, memory, time of execution) needed to reproduce the experiments?

Answer: [Yes]

Justification: Details about resources and implementation are provided in Appendix D.1.

Guidelines:

- The answer [N/A] means that the paper does not include experiments.
- The paper should indicate the type of compute workers CPU or GPU, internal cluster, or cloud provider, including relevant memory and storage.
- The paper should provide the amount of compute required for each of the individual experimental runs as well as estimate the total compute.
- The paper should disclose whether the full research project required more compute than the experiments reported in the paper (e.g., preliminary or failed experiments that didn't make it into the paper).

#### 9. Code of ethics

Question: Does the research conducted in the paper conform, in every respect, with the NeurIPS Code of Ethics <https://neurips.cc/public/EthicsGuidelines?>

Answer: [Yes]

Justification: Yes, the research conducted in this paper conforms in every respect with the NeurIPS Code of Ethics.

Guidelines:

- The answer [N/A] means that the authors have not reviewed the NeurIPS Code of Ethics.
- If the authors answer [No], they should explain the special circumstances that require a deviation from the Code of Ethics.
- The authors should make sure to preserve anonymity (e.g., if there is a special consideration due to laws or regulations in their jurisdiction).

#### 10. Broader impacts

Question: Does the paper discuss both potential positive societal impacts and negative societal impacts of the work performed?

Answer: [Yes]

Justification: The broader impact of our work is discussed in Appendix F.

Guidelines:

- The answer [N/A] means that there is no societal impact of the work performed.
- If the authors answer [N/A] or [No], they should explain why their work has no societal impact or why the paper does not address societal impact.
- Examples of negative societal impacts include potential malicious or unintended uses (e.g., disinformation, generating fake profiles, surveillance), fairness considerations (e.g., deployment of technologies that could make decisions that unfairly impact specific groups), privacy considerations, and security considerations.
- The conference expects that many papers will be foundational research and not tied to particular applications, let alone deployments. However, if there is a direct path to any negative applications, the authors should point it out. For example, it is legitimate to point out that an improvement in the quality of generative models could be used to generate Deepfakes for disinformation. On the other hand, it is not needed to point out that a generic algorithm for optimizing neural networks could enable people to train models that generate Deepfakes faster.
- The authors should consider possible harms that could arise when the technology is being used as intended and functioning correctly, harms that could arise when the technology is being used as intended but gives incorrect results, and harms following from (intentional or unintentional) misuse of the technology.
- If there are negative societal impacts, the authors could also discuss possible mitigation strategies (e.g., gated release of models, providing defenses in addition to attacks, mechanisms for monitoring misuse, mechanisms to monitor how a system learns from feedback over time, improving the efficiency and accessibility of ML).

## 11. Safeguards

Question: Does the paper describe safeguards that have been put in place for responsible release of data or models that have a high risk for misuse (e.g., pre-trained language models, image generators, or scraped datasets)?

Answer: [Yes]

Justification: Our work focuses on hallucination detection in LLMs, which does not introduce new safety risks but rather contributes to mitigating them. No new models or datasets are released as part of this work.

Guidelines:

- The answer [N/A] means that the paper poses no such risks.
- Released models that have a high risk for misuse or dual-use should be released with necessary safeguards to allow for controlled use of the model, for example by requiring that users adhere to usage guidelines or restrictions to access the model or implementing safety filters.
- Datasets that have been scraped from the Internet could pose safety risks. The authors should describe how they avoided releasing unsafe images.
- We recognize that providing effective safeguards is challenging, and many papers do not require this, but we encourage authors to take this into account and make a best faith effort.

## 12. Licenses for existing assets

Question: Are the creators or original owners of assets (e.g., code, data, models), used in the paper, properly credited and are the license and terms of use explicitly mentioned and properly respected?

Answer: [Yes]

Justification: Yes, we appropriately credit the authors and licenses for all models, methods, and datasets utilized in this paper.

Guidelines:

- The answer [N/A] means that the paper does not use existing assets.
- The authors should cite the original paper that produced the code package or dataset.

- The authors should state which version of the asset is used and, if possible, include a URL.
- The name of the license (e.g., CC-BY 4.0) should be included for each asset.
- For scraped data from a particular source (e.g., website), the copyright and terms of service of that source should be provided.
- If assets are released, the license, copyright information, and terms of use in the package should be provided. For popular datasets, [paperswithcode.com/datasets](https://paperswithcode.com/datasets) has curated licenses for some datasets. Their licensing guide can help determine the license of a dataset.
- For existing datasets that are re-packaged, both the original license and the license of the derived asset (if it has changed) should be provided.
- If this information is not available online, the authors are encouraged to reach out to the asset’s creators.

### 13. **New assets**

Question: Are new assets introduced in the paper well documented and is the documentation provided alongside the assets?

Answer: [N/A]

Justification: The paper does not release new datasets or models.

Guidelines:

- The answer [N/A] means that the paper does not release new assets.
- Researchers should communicate the details of the dataset/code/model as part of their submissions via structured templates. This includes details about training, license, limitations, etc.
- The paper should discuss whether and how consent was obtained from people whose asset is used.
- At submission time, remember to anonymize your assets (if applicable). You can either create an anonymized URL or include an anonymized zip file.

### 14. **Crowdsourcing and research with human subjects**

Question: For crowdsourcing experiments and research with human subjects, does the paper include the full text of instructions given to participants and screenshots, if applicable, as well as details about compensation (if any)?

Answer: [N/A]

Justification: This work does not involve crowdsourcing or research with human subjects.

Guidelines:

- The answer [N/A] means that the paper does not involve crowdsourcing nor research with human subjects.
- Including this information in the supplemental material is fine, but if the main contribution of the paper involves human subjects, then as much detail as possible should be included in the main paper.
- According to the NeurIPS Code of Ethics, workers involved in data collection, curation, or other labor should be paid at least the minimum wage in the country of the data collector.

### 15. **Institutional review board (IRB) approvals or equivalent for research with human subjects**

Question: Does the paper describe potential risks incurred by study participants, whether such risks were disclosed to the subjects, and whether Institutional Review Board (IRB) approvals (or an equivalent approval/review based on the requirements of your country or institution) were obtained?

Answer: [N/A]

Justification: Not applicable, as this work does not involve human subjects or study participants.

Guidelines:

- The answer [N/A] means that the paper does not involve crowdsourcing nor research with human subjects.
- Depending on the country in which research is conducted, IRB approval (or equivalent) may be required for any human subjects research. If you obtained IRB approval, you should clearly state this in the paper.
- We recognize that the procedures for this may vary significantly between institutions and locations, and we expect authors to adhere to the NeurIPS Code of Ethics and the guidelines for their institution.
- For initial submissions, do not include any information that would break anonymity (if applicable), such as the institution conducting the review.

#### 16. Declaration of LLM usage

Question: Does the paper describe the usage of LLMs if it is an important, original, or non-standard component of the core methods in this research? Note that if the LLM is used only for writing, editing, or formatting purposes and does *not* impact the core methodology, scientific rigor, or originality of the research, declaration is not required.

Answer: [N/A]

Justification: LLMs are the subject of analysis in this work but are not used as part of the research methodology in a novel or non-standard way, in accordance with the LLM policy in the NeurIPS handbook. Their usage is limited to evaluation and does not constitute an original component of the core methodology.

Guidelines:

- The answer [N/A] means that the core method development in this research does not involve LLMs as any important, original, or non-standard components.
- Please refer to our LLM policy in the NeurIPS handbook for what should or should not be described.